

Origin and evolution of turiasaur dinosaurs set by means of a new ‘rosetta’ specimen from Spain

RAFAEL ROYO-TORRES^{1,*}, ALBERTO COBOS¹, PEDRO MOCHO^{2,3} and LUIS ALCALÁ¹

¹Fundación Conjunto Paleontológico de Teruel-Dinópolis / Museo Aragonés de Paleontología, avenida Sagunto s/n 44002 Teruel, Spain

²Instituto Dom Luiz, Universidade de Lisboa, Edifício C6, Campo Grande, 1749-016 Lisboa, Portugal

³Grupo de Biología Evolutiva, UNED, Facultad de Ciencias, UNED, Paseo Senda del Rey 9, 28040 Madrid, Spain

Received 21 November 2019; revised 6 July 2020; accepted for publication 13 July 2020

Turiasauria is a non-neosauropod eusauropod clade of dinosaurs known since 2006, when the description of *Turiasaurus* was published. This group, including *Losillasaurus*, was originally thought to have been restricted to the Late Jurassic of Spain. However, over the last decade, our knowledge of this group has improved with the discovery of new taxa such as *Zby* from the Portuguese Late Jurassic, *Tendaguria* from the Tanzanian Late Jurassic and *Mierasaurus* and *Moabosaurus* from the Early Cretaceous of the USA. Here, we describe a new specimen of *Losillasaurus* from Spain, which allows us to better understand the character variation in the cranial and postcranial skeleton. The review of some sauropod fauna of Madagascar, and inclusion of some specimens of Turiasauria, suggest that this clade might have arisen in the Middle Jurassic. According to our phylogenetic results, a specimen found in the early 19th century in Madagascar is shown to be the oldest and only member of Turiasauria represented in the Middle Jurassic thus far. This is named *Narindasaurus thevenini* **gen. & sp. nov.** Turiasauria is thus known from the Middle Jurassic in Pangaea, diversified in the Late Jurassic in Gondwana and Laurasia, and dispersed during the Early Cretaceous to North America.

ADDITIONAL KEYWORDS: Cretaceous – Jurassic – Sauropodomorpha – Laurasia – Gondwana – Dinosauria – origins – phylogenetic systematics.

INTRODUCTION

The Turiasauria clade represents a group of sauropod dinosaurs with a wide geographic distribution across Europe, North America and Africa (Royo-Torres *et al.*, 2017; Mannion *et al.*, 2019). This clade is known thanks to the study of the sauropod dinosaur *Turiasaurus riodevensis* Royo-Torres *et al.*, 2006 found in Riodeva (Teruel province, south of the Iberian Range, Spain). *Turiasaurus* Royo-Torres *et al.*, 2006 is defined by the representative cranial (Fig. 1A) and postcranial remains found from 2003 onwards in the Villar del Arzobispo Formation (Luque *et al.*, 2005; Royo-Torres *et al.*, 2006; Royo-Torres & Upchurch,

2012), currently dated as Kimmeridgian–Tithonian (Campos Soto *et al.*, 2019). Aside from the specimens of turiasaurs from Teruel, other Late Jurassic sauropod fossils from the Iberian Peninsula have been assigned to the Turiasauria clade, including two other taxa: *Losillasaurus giganteus* Casanovas *et al.*, 2001 and *Zby atlanticus* Mateus *et al.*, 2014. *Losillasaurus* Casanovas *et al.*, 2001 was found at the La Cañada site (Losilla de Aras, Valencia) and originates from the same geological unit as *Turiasaurus* (Casanovas *et al.*, 2001; Royo-Torres *et al.*, 2006). This taxon was only known from a partial braincase and postcranial material (Casanovas *et al.*, 2001), but here we describe new material from another specimen (Supporting Information, File S1). We provide new information on the anterior part of the skull (Figs 1, 2), which includes details key to understanding the tooth variation in turiasaurs. *Zby atlanticus* from the Vale de Pombas site (Lourinhã), Lusitanian Basin in

*Corresponding author. E-mail: royo@dinopolis.com

[Version of record, published online 3 September 2020; <http://zoobank.org/> urn:lsid:zoobank.org:act:B7203900-1F11-40CD-B4D5-115BAD1B96FE]

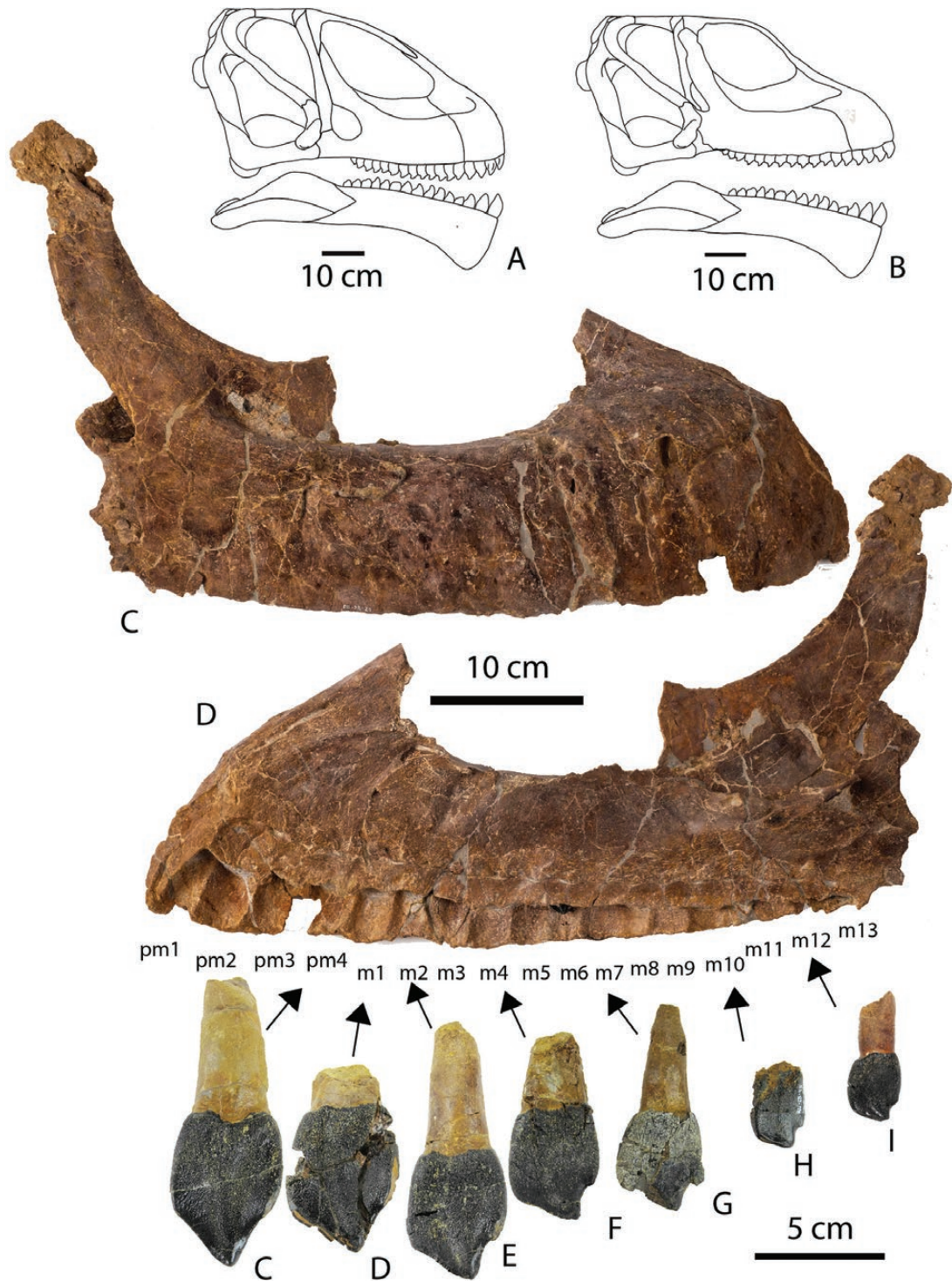


Figure 1. Reconstructions of the skull of *Turiasaurus* (A) and *Losillasaurus* (B) in the lateral view. Left premaxilla, maxilla and teeth (MAP-6005) of *Losillasaurus giganteus* (San Lorenzo specimen) in labial or lateral (C) and lingual or medial (D) views. Right premaxillary tooth (MAP-6013) (E); and right maxillary teeth (MAP-6014) (F), (MAP-6015) (G), (MAP-6016) (H), (MAP-6017) (I), (MAP-6018) (J), (MAP-6019) (K) in lingual views.

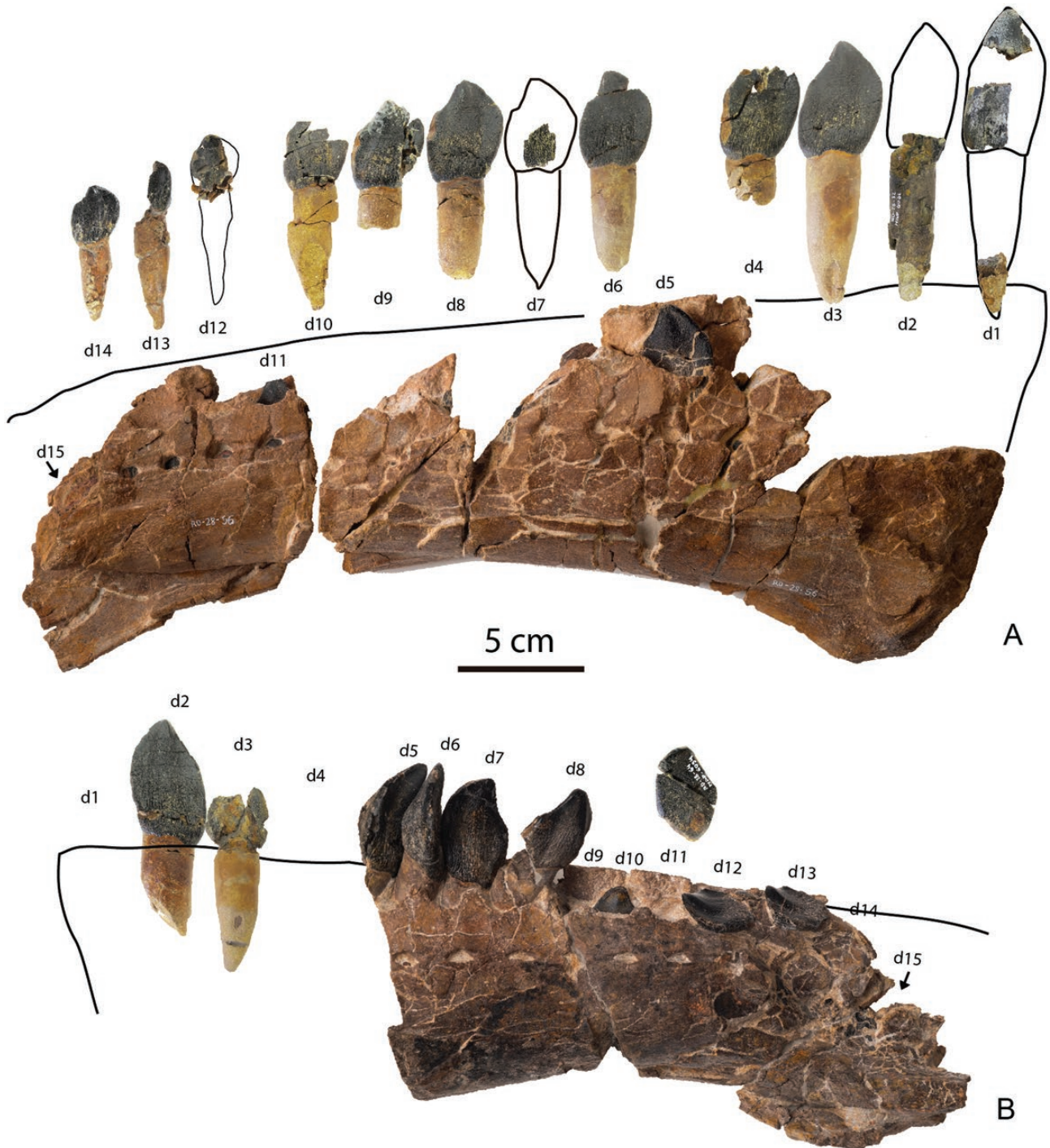


Figure 2. Left dentary and teeth (MAP-6008) of *Losillasaurus giganteus* (San Lorenzo specimen) in lingual view (A); left dentary teeth (MAP-6045) (d1), (MAP-6031) (d2), (MAP-6035) (d3), (MAP-6037) (d4), (MAP-6036) (d7), (MAP-6038) (d8), (MAP-6039) (d9), (MAP-6040) (d10), (MAP-6020) (d13), (MAP-6021) (d14) in lingual views. Right dentary and teeth (MAP-6009) of *Losillasaurus giganteus* (San Lorenzo specimen) in lingual view (B). Right dentary teeth (MAP-6032) (d2) and (MAP-6033) (d3) of *Losillasaurus giganteus* (San Lorenzo specimen) in lingual view.

Portugal, has been described with a tooth and forelimb dated as Late Kimmeridgian (Mateus *et al.*, 2014). In the European domain, Schwarz *et al.* (2020) proposed the taxa *Amanzia greppini* (von Huene, 1922) from Switzerland as a possible member of Turiasauria. Recent studies also suggest a wider palaeogeographic distribution and stratigraphic range for Turiasauria extending to North America (Royo-Torres *et al.*, 2017) with *Mierasaurus* Royo-Torres *et al.*, 2017 and *Moabosaurus* Britt *et al.*, 2017, and Africa (Mannion *et al.*, 2019) with *Tendaguria* Wild, 1991. Our work describes a new turiasaur specimen from Spain, defines a new genus and species as a result of the review of historical material from Madagascar, and updates the characters to support the Turiasauria clade.

MATERIAL AND METHODS

We have been working on the excavation of the new specimen from the San Lorenzo site in Riodeva (Teruel, Spain) since 2010. We also provided special supervision of the laboratory preparation and conditioning of the exhibition fossils for the Dinópolis Museum (Teruel) in the Dinosaur Hall. We visited every institution with identified or purported turiasaurs in Spain, Portugal, France, the UK, Germany, the USA and Argentina. The specimens studied are housed in different museums (see Supporting Information, File S1) and all were studied by us first-hand. We prepared the measurements (see Supporting Information, Files S2–S4) and pictures.

Material from the San Lorenzo site (Riodeva, Teruel, Spain) in the Villar del Arzobispo Formation (Kimmeridgian–Tithonian) is described in this work. It was initially only known by a caudal vertebra (Royo-Torres *et al.*, 2009) until a partial skeleton was recovered after excavation work in 2010 and 2011 (Cobos *et al.*, 2011). It consists of a cranial and postcranial skeleton (for a list of bones see Supporting Information, File S1). Another specimen identified in this work is a complete anterior caudal vertebra (SHN (JJS) 180) from Baleal (Peniche, Portugal), Praia de Amoreira-Porto Novo Formation dated to the Upper Kimmeridgian–Lower Tithonian (Mocho *et al.*, 2017b). The third specimen studied in this work are remains (for a list of bones see Supporting Information, File S1) located at the Ankinganivalaka municipality on the right bank of a meander of the Loza River in the Middle Isalo III Formation (Bathonian) (Lemoine, 1906; Besairie & Collignon, 1972; Läng, 2008; Mannion, 2010).

ANALYTICAL PROTOCOL FOR THE PHYLOGENETIC ANALYSES

While there is a consensus regarding the monophyly of the Turiasauria clade, which includes *Losillasaurus*,

Mierasaurus, *Moabosaurus*, *Tendaguria*, *Turiasaurus*, *Zby*, (Royo-Torres *et al.*, 2017; Mannion *et al.*, 2019) and probably *Amanzia* (Schwarz *et al.*, 2020), the relative phylogenetic position between them is still debated. We investigated their position via an updated version of the largest available data matrix for sauropods (Mannion *et al.*, 2019; Schwarz *et al.*, 2020), which included all turiasaur taxa and the new material from San Lorenzo referred to here to *Losillasaurus*. In addition, in order to test the potential close relationship of taxa from the Middle Jurassic of Madagascar (Läng, 2008) (see Systematic Palaeontology section) with the Turiasauria clade (Mocho *et al.*, 2016), we included these Madagascar taxa in the phylogenetic analyses. The final dataset comprises 118 taxa scored for 542 characters with some modifications for *Losillasaurus* and *Turiasaurus* due to the new elements included in these taxa (see Supporting Information, File S1). We provide our full data matrix in MESQUITE and TNT file formats (Supporting Information, Files S5, S6). Characters 11, 14, 15, 27, 40, 51, 104, 122, 147, 148, 195, 205, 259, 297, 426, 435, 472 and 510 were treated as ordered multistate characters, as in Mannion *et al.* (2019). Following previous versions of this data matrix, and the preliminary analyses, several fragmentary and unstable taxa were identified and excluded a priori (Mannion *et al.*, 2017; Mannion *et al.*, 2019; Schwarz *et al.*, 2020) (for information about codification see Supporting Information, File S1).

RESULTS

DESCRIPTION AND COMPARISON OF A NEW GIANT SPECIMEN OF SPANISH TURIASAUR FROM THE VILLAR DEL ARZOBISPO FORMATION (KIMMERIDGIAN–TITHONIAN)

Premaxilla–maxilla

An articulated right premaxilla and maxilla (MAP-6005, see institutional abbreviations in Supporting Information, File S1) are preserved, although the ascending process of the premaxilla is broken just after its base (Fig. 1C, D). The ascending process in lateral view is seen to be slightly concave, as in *Mamenchisaurus* Young, 1954 (Ouyang & Ye, 2002), and it probably has a large dorsal projection. It is a robust premaxilla with a subrectangular shape in lateral view and has four functional teeth. The anterior margin gives a short ‘muzzle’ without a step, and the contact with the maxilla is straight. The external surface has an anteroventrally orientated vascular groove originating from the contact with the maxilla. The maxilla is rectangular in shape and long anteroposteriorly with 13 dental alveoli. The

maxillary tooth row ends anterior to the preserved portion of the antorbital fenestra, a feature also present in diplodocoids (Upchurch, 1998; Wilson, 2002, 2005). The posterior end of the body is a little less robust than the anterior end. The dorsal ascending process is flat and thin, different to that of *Turiasaurus*, and slopes strongly posterodorsally to likely contact the upper end of the lacrimal. The preserved margins of the antorbital fenestra infer a small fenestra, smaller than that of *Turiasaurus* (Fig. 1). The lateral surface of the premaxilla and maxilla has dorsoventrally elongated grooves. A derived feature only described in diplodocoids (*Apatosaurus* Marsh, 1877, *Diplodocus* Marsh, 1878, *Dicraeosaurus* Janensch, 1914 and *Nigersaurus* Sereno *et al.*, 1999) and *Nemegtosaurus* Nowinski, 1971 (Wilson, 2005; Tshopp *et al.*, 2015; Mannion *et al.*, 2019). It is considered a synapomorphy of Dicraeosauridae (Mannion *et al.*, 2012; Tshopp *et al.*, 2015). This feature may be a diagnostic character for this turiasaur genus, because it is absent in the *Turiasaurus* and *Mierasaurus* skulls. The tooth formula is four premaxillary and 13 maxillary teeth.

Dentary

The left and right dentaries (MAP-6008 and MAP-6009) have been preserved (Fig. 2). They consist of thick vertical plates of bone, the posterior two-thirds of which lie in a parasagittal plane, while the anterior portion curves slightly to meet its partner at the symphysis. The anterior end of the dentary is bent downwards so that the long-axis of the symphysis forms an angle of 110° to the long-axis of the mandible. The cross-sectional shape of symphysis is oblong and the anteroventral margin of the dentary is gently rounded in shape. Each alveolus has two or three replacement teeth. The dentary has a longitudinal groove going from the lingual position in the chin to the posterior end on the ventral surface. There are 15 alveoli for the left dentary teeth, which decrease in size as they progress posteriorly.

Dentition

The San Lorenzo specimen has several teeth in anatomical position (Figs 1, 2; see Supporting Information, File S3 for measurements): two unerupted teeth in the right premaxillary–maxillary bones, seven teeth in the right dentary and two teeth in the left dentary. Thirty isolated teeth have been referred to the same specimen. Regarding morphology, namely the shape and size of the teeth in articulation with the skull, each isolated tooth has been placed in the left or right dentaries or maxillae/premaxillae.

As in other sauropods such as *Camarasaurus* Cope, 1877 (Wiersma & Sander, 2017), the tooth crowns gradually decrease in size, being larger mesially and smaller distally. In the mesialmost region, the crown apex is apically oriented to the base of the crown. These are the premaxillary teeth (Figs 1, 3) and anteriormost teeth in the dentary (Figs 2, 4). In the case of the dentary, from d3 to d15 (Fig. 2) and the maxillary teeth, the apices move to the more distal region and become apicodistally oriented. This leads to a more distally shifted apex with an asymmetric appearance in the mesiodistal view. In general, every tooth has a convex labial crown face and concave lingual face. This asymmetric feature makes it possible to assign isolated teeth to the right or left side of the skull. However, we need the help of another feature to assign isolated teeth to either the maxillary or dentary. When looking at the teeth in mesial or distal view, the crown is curved linguallly in both the premaxillary and maxillary teeth, and the crown is directed towards the labial in the dentary teeth (Figs 3, 4). This anatomical difference allows us to set the teeth in the skull, and this criterion may be applicable to other groups of sauropods. Furthermore, it has been confirmed in *Turiasaurus* and in a thus far unpublished specimen referred to *Camarasaurus* from Colorado (CPT-4445 to CPT-4460). These features were also described in *Camarasaurus* (Carey & Madsen, 1972; Wiersma & Sander, 2017), *Diplodocus*, *Europasaurus* Mateus *et al.*, 2006 (Wiersma & Sander, 2017), *Giraffatitan* Paul, 1988, *Nemegtosaurus* and *Quaesitosaurus* Kurzanov & Bannikov, 1983 (Upchurch, 1998; Upchurch *et al.*, 2004a). The tooth distribution in the skull of the San Lorenzo specimen consists of four alveoli in the premaxillae, 13 in the maxillae and 15 in each dentary. In contrast to neosauropods, which are described as homodont (McIntosh *et al.*, 1996; Chatterjee & Zheng, 2005; Wiersma & Sander, 2017), turiasaurs have a heterodont dentition, such as *Turiasaurus* (Royo-Torres & Upchurch, 2012) and *Mierasaurus* (Royo-Torres *et al.*, 2017). Previous studies described three morphotypes for the heart-shaped teeth of this clade (Mocho *et al.*, 2016, 2017a). However, thanks to the teeth in the skull of the San Lorenzo specimen, we can identify the correct anatomical position for each morphotype in the skull. This leads to the identification of four types of tooth morphology: (1) anterior dentary teeth, (2) middle and posterior dentary teeth, (3) premaxillary teeth and (4) maxillary teeth. In general, each tooth crown in this specimen has a labiolingually compressed heart/spoon-shaped morphology and presents enamel with a wrinkled texture. This texture is produced by a set of small scales. The teeth are different to those of

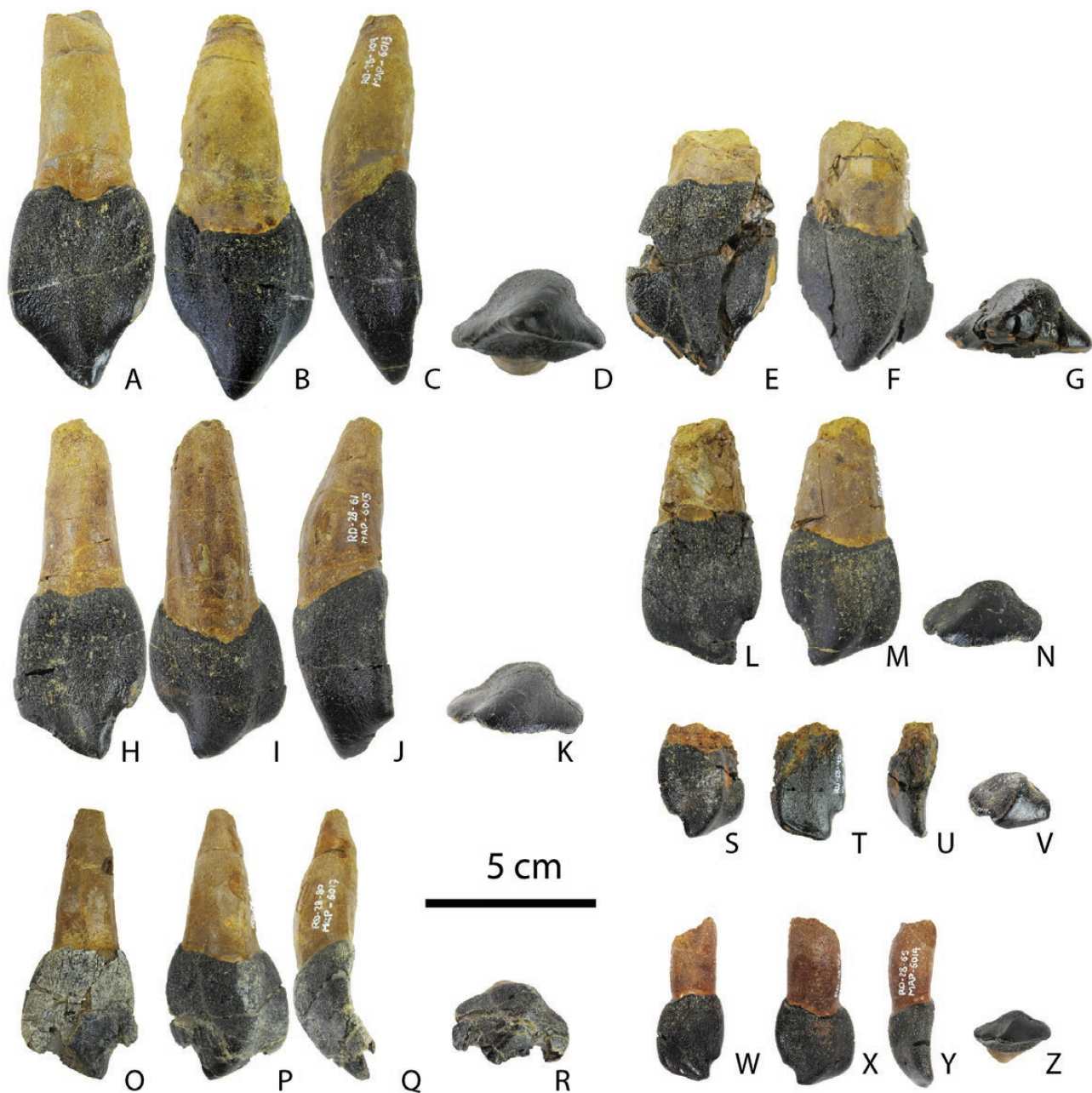


Figure 3. Right premaxillary and maxillary teeth of *Losillasaurus giganteus* (San Lorenzo specimen): premaxillary teeth (MAP-6013) in lingual (A), labial (B), mesial (C) and apical (D) views; maxillary teeth (MAP-6014) in lingual (E), labial (F) and apical (G) views; maxillary teeth (MAP-6015) in lingual (H), labial (I), mesial (J) and apical (K) views; maxillary teeth (MAP-6016) in lingual (L), labial (M) and apical (N) views; maxillary teeth (MAP-6017) in lingual (O), labial (P), mesial (Q) and apical (R) views; maxillary teeth (MAP-6018) in labial (S), lingual (T), mesial (U) and apical (V) views; and maxillary teeth (MAP-6019) in lingual (W), labial (X), mesial (Y) and apical (Z) views.

Turiasaurus, which are acicular and whose wrinkled texture features more complex scales. The wrinkles are most prominent on the labial surface, similar to the teeth of *Turiasaurus* (Royo-Torres & Upchurch, 2012), namely on the bulge area and near the base of the crown (Mocho *et al.*, 2017a). In general, the

crown is slightly apicomesially projected and the teeth reach the maximum mesiodistal width near the base of the apex. On the labial face, the teeth display an apicobasal bulge bounded by two shallow grooves (Fig. 6) with the same orientation. The lingual face has a low apicobasal ridge, which may extend along the

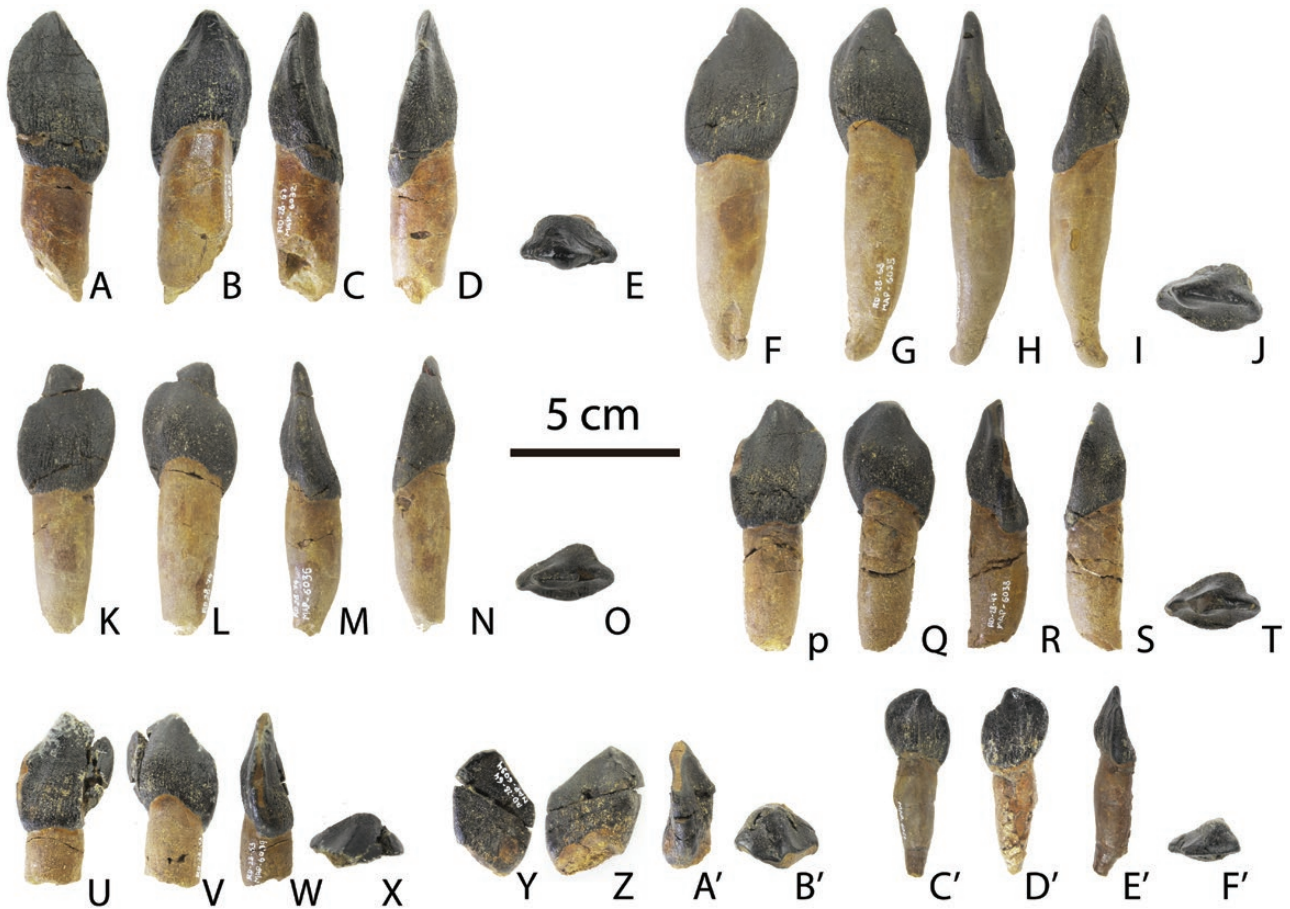


Figure 4. Dendary teeth of *Losillasaurus giganteus* (San Lorenzo specimen): right dendary teeth (MAP-6032) in lingual (A), labial (B), mesial (C), distal (D) and apical (E) views; left dendary teeth (MAP-6035) in lingual (F), labial (G), distal (H), mesial (I) and apical (E) views; left dendary teeth (MAP-6036) in lingual (K), labial (L), distal (M), mesial (N) and apical (O) views; left dendary teeth (MAP-6038) in lingual (P), labial (Q), distal (R), mesial (S) and apical (T) views; left dendary teeth (MAP-6039) in lingual (U), labial (V), distal (W) and apical (X) views; right dendary teeth (MAP-6034) in lingual (Y), labial (Z), distal (A') and apical (B') views; and left dendary teeth (MAP-6021) in labial (C'), lingual (D'), distal (E') and apical (F') views.

entire apicobasal length. It occupies the central part of the lingual concavity. The lingual crest is variable and sometimes reaches the base of the crown where it develops a flat-to-convex mesiodistal platform. The mesial and distal edges of the crown are not parallel and diverge from the base of the tooth. The transition between the root and crown is well defined in every tooth. The teeth exhibit an asymmetrical 'D'-shaped cross-section with a convex labial face and flat-to-smooth concave lingual face. The asymmetrical apex deflects distally and could bear mesial, distal and apical facets, depending on the development of wear. Except for in the premaxillary teeth (see below), the mesial edge of the apex is convex, while the distal edge is concave in the labial and lingual views. Crown-to-crown occlusion produced 'V'-shaped wear facets. At the tip of the apex, the surface is smoother as in other

sauropod teeth (i.e. *Amygdalodon* Cabrera, 1947; Carballido & Pol, 2010). Unworn crowns typically lack serrations, except in the d2 (MAP-6032), where a couple of rounded denticles are seen in the mesial apex boundary. The roots are slightly labiolingually compressed cones that are mesiodistally narrower than the base of the crown. They have several smooth apicobasal grooves: three in the dendary teeth (Fig. 5), two in the labial face and one in the lingual face. They are similar to the roots of the dendary teeth of *Turiasaurus*. Some dendary teeth have up to four grooves, i.e. MAP-6033, although the usual amount is three (Fig. 5 B, C; MAP-6035). The roots of the premaxillary and maxillary teeth usually have six low apicobasal grooves (unknown in *Turiasaurus*): four grooves in the labial face and two in the lingual face, namely MAP 6013 (Fig. 5A).

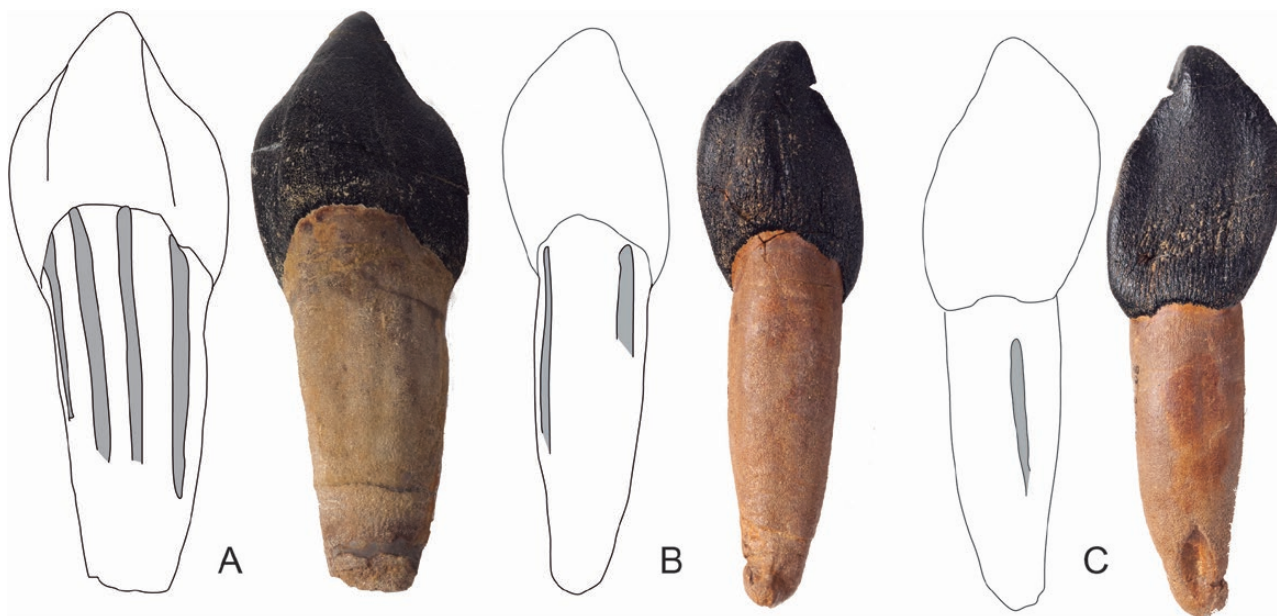


Figure 5. Longitudinal grooves in the right premaxillary teeth (MAP-6013) in the labial view (A) and left dentary teeth (MAP-6035) in labial (B) and lingual (C) views of *Losillasaurus giganteus* (San Lorenzo specimen).

Premaxillary teeth

The four premaxillary teeth (MAP-6013) are bent lingually and their crowns are curved in the same direction (Figs 1, 3). They are the most robust teeth, labiolingually longer compared to the other teeth (see Supporting Information, File S3) and have a symmetric heart-shape appearance. The mesial and distal edges of the apex are both slightly concave in the labial and lingual views. The SI values of this morphotype are close to 1.33 (Pm4, MAP-6013). The lingual face is apicobasally concave and flat-to-concave mesiodistally with a platform at the base of the crown.

Maxillary teeth

There are 13 maxillary teeth (Figs 1, 3; Supporting Information, File S3). They are bent lingually and the asymmetric crown is also curved lingually. They have a well-defined heart-shaped outline, an apicomésially projected crown and a pronounced curvature of the apex. The maxillary teeth are diagnostic. The apex is shorter (apex/crown height ratio 0.3–0.24) than the apex of *Turiasaurus* (CPT-3941, apex/crown height ratio 0.4) (Fig. 6). In addition, the teeth of the San Lorenzo specimen have a ‘secondary apex’ on the distal edge in the transition between the apex and base of the crown (Figs 1, 3). This ‘secondary apex’ is considered a potential autapomorphy and is unknown in any other sauropod. The mesial and distal edges of the main apex are straight and concave, respectively. The shape of the maxillary teeth is between that of a

heart and rounded square, and they are labiolingually more compressed and shorter than the other teeth. The maxillary teeth have intermediate SI values of 1.3–1.07. The lingual face is apicobasally concave and flat-to-concave mesiodistally with a platform at the base of the crown. On the labial face, the maxillary teeth of the San Lorenzo specimen display an apicobasal bulge bounded by two shallow grooves with the same orientation, while *Turiasaurus* has only one labial groove on the mesial edge (Fig. 6).

Dentary teeth

The 15 dentary teeth (Figs 2, 4; Supporting Information, File S3) decrease in size as they progress posteriorly. The teeth curve labially and the crown is also directed labially. The first and second mesialmost dentary teeth differ from the middle and distalmost dentary teeth. They have heart-shaped crowns, which are more apicobasally elongated and labiolingually compressed than the posterior dentary teeth. They also have higher SI values: 1.73 in d2, and ranging from 1.18 to 1.53 in d3 to d15. In the mesialmost teeth, the mesial and distal edges at the base of the crown are closely parallel and straighter than in the other dentary teeth. In d1 and d2, the apex is particularly long and presents a slight distal deflection, which is not as pronounced as in the posterior dentary teeth. The distal edge of the apex is concave, while the mesial edge is convex-to-straight. The middle and distalmost dentary teeth have a well-defined heart-shaped outline,

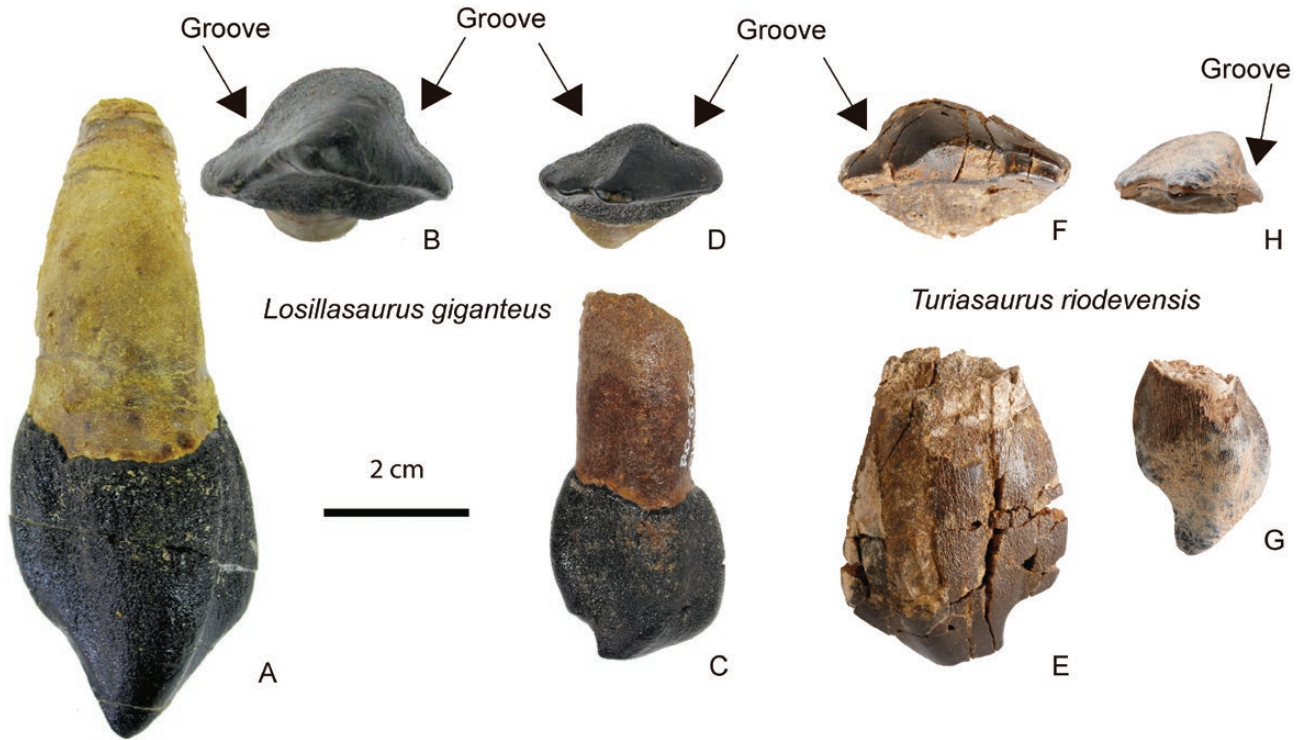


Figure 6. Comparison between *Turiasaurus* and *Losillasaurus* teeth: right premaxillary teeth (MAP-6013) in labial (A) and apical (B) views of *Losillasaurus giganteus* (San Lorenzo specimen); right maxillary teeth (MAP-6019) in labial (C) and apical (D) views of *Losillasaurus giganteus* (San Lorenzo specimen); left maxillary teeth (CPT-1262) in labial (E) and apical (F) views of *Turiasaurus riodevensis*; left maxillary teeth (CPT-3941) in labial (G) and apical (H) views of *Turiasaurus riodevensis*.

an apicomésially projected crown, and a pronounced curvature of the apex.

Dorsal vertebra and rib

Only one dorsal vertebral fragment (MAP-6047) is preserved in the San Lorenzo specimen. It comprises the neural spine, transverse lateral processes, one prezygapophysis and hyposphene. This fragment likely belongs to a middle dorsal vertebra compared to the dorsal vertebrae of *Turiasaurus*. It lacks the anchor morphology seen in *Turiasaurus* (Fig. 7). A dorsal rib (MAP-6048) was found, which is probably related to a posterior vertebra, although it may be related to the preserved fragment. It displays a long capitulum and short tuberculum with solid bone in its interior. The neck lacks pneumatic cavities or foramina, but there is one in the proximal surface of the tuberculum.

Caudal vertebrae

In total, 35 caudal vertebrae belonging to this specimen (CPT-1846a and b, MAP-6050 to MAP-6083) have been recovered (Figs 8–10; Supporting Information, File S3).

They represent the fourth to 38th vertebrae in the caudal series. In addition, the last preserved caudal vertebra is interpreted as a distal caudal vertebra, likely located between the 40th and 50th caudal vertebrae. The length for the caudal centra is approximately the same in the first 15 preserved caudal vertebrae, and the caudal transverse processes persist through 15 vertebrae. According to the holotype specimen of *Losillasaurus*, for which it is possible to study the first five caudal vertebrae (Casanovas *et al.*, 2001), the first complete caudal vertebra from the San Lorenzo specimen should be the sixth. Both the fifth (type specimen) and sixth vertebrae (San Lorenzo specimen) are similar in morphology, but differ slightly in articulation: the fifth is more convex posteriorly than the sixth caudal vertebra. The sixth caudal centrum is flat and slightly convex on the posterior surface, displaying variable concavity in the central area of the articulation, which becomes barely perceptible from the sixth caudal vertebra onwards. Thus, the anterior caudal articular surfaces are slightly procoelous. This feature is differentiated from the strong convex posterior articulations of titanosaurs and mamenchisaurids such as *Wamweracaudia* Mannion *et al.*, 2019 (HMN

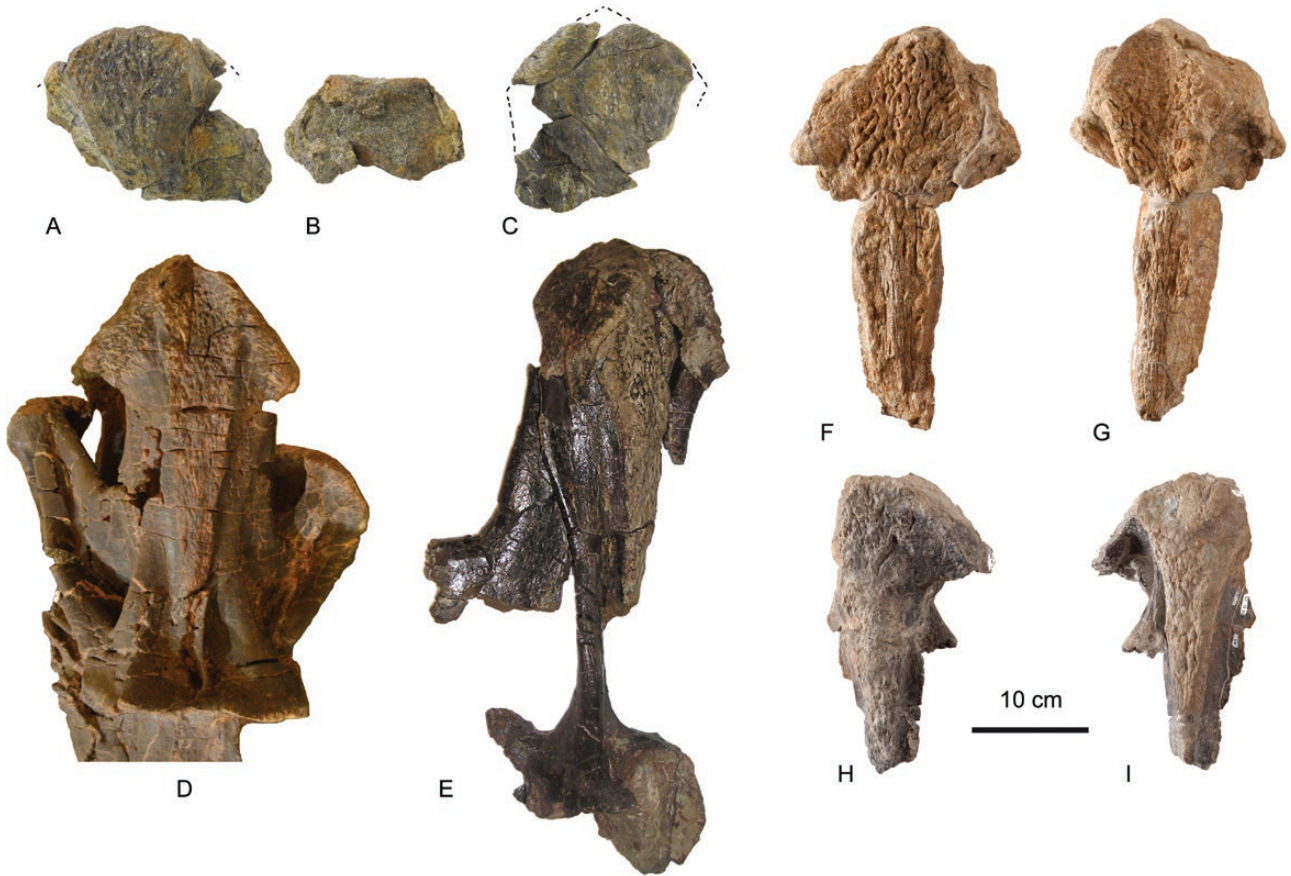


Figure 7. Dorsal spines (MAP-6047) of *Losillasaurus giganteus* (San Lorenzo specimen) in anterior (A), dorsal (B) and posterior views. Dorsal spines (MCNV Lo-11) of *Losillasaurus giganteus* (paratype) in posterior view (D). Dorsal spines (MCNV Lo-17b) of *Losillasaurus giganteus* (paratype) in posterior view (E). Dorsal spine (CPT-2688) of *Turiasaurus riodevensis* (paratype) in posterior (F) and anterior (G) views. Dorsal spine (CPT-1633) of *Turiasaurus riodevensis* (referred to material) in posterior (H) and anterior (I) views.

MB.R.2901.1–30) (Mannion *et al.*, 2019). The middle caudal vertebrae are amphicoelous, with the anterior cup moderately deeper than the posterior one. The posterior and distal caudal vertebrae are procoelous with the posterior surface completely covered by the convexity. The latter differs from the opisthocelous condition seen in *Turiasaurus* (Royo-Torres *et al.*, 2006). Rugosity is present in the dorsal half of the posterior articulation surface between the sixth and eighth caudal vertebrae, and a small concavity appears posteriorly in the same area. There is a horizontal notch in a similar position in the 23rd to 27th caudal vertebrae. The caudal bone texture is solid in all vertebrae, meaning they lack pneumatic fossae and foramina. The transverse processes extend from the neural arch to lateral face of the centrum in the anterior caudal vertebrae, with a triangular distal taper in the anterior and posterior views. They are directed posteriorly and dorsally. This characteristic differs in the caudal vertebrae of *Turiasaurus*, where

the transverse processes are directed laterally or anterolaterally. In the middle caudal vertebrae (from the 11th to 14th caudal vertebrae) of the San Lorenzo specimen (RD-28), they do not reach the posterior margin of the centrum, and it is thus different from the condition for basal Titanosauriformes (D’Emic, 2012). The lateral processes are rectangular and compressed dorsoventrally in the dorsal and ventral views. The neural arch in the anterior and middle caudal vertebrae is located on the anterior half of the centrum. The caudal neural spine is transversely compressed and has a dorsoventrally short spinopostzygapophyseal fossa. This character is similar to that found in basal eusauropods and basal macronarians. They have a relatively short neural spine for anterior caudal vertebrae, resembling the condition present in *Giraffatitan* (Janensch, 1950). In the anterior caudal vertebrae, the spinoprezygapophyseal lamina is present at the base of the spine and disappears into the lateral surface of the neural spine. The anterior surface of the

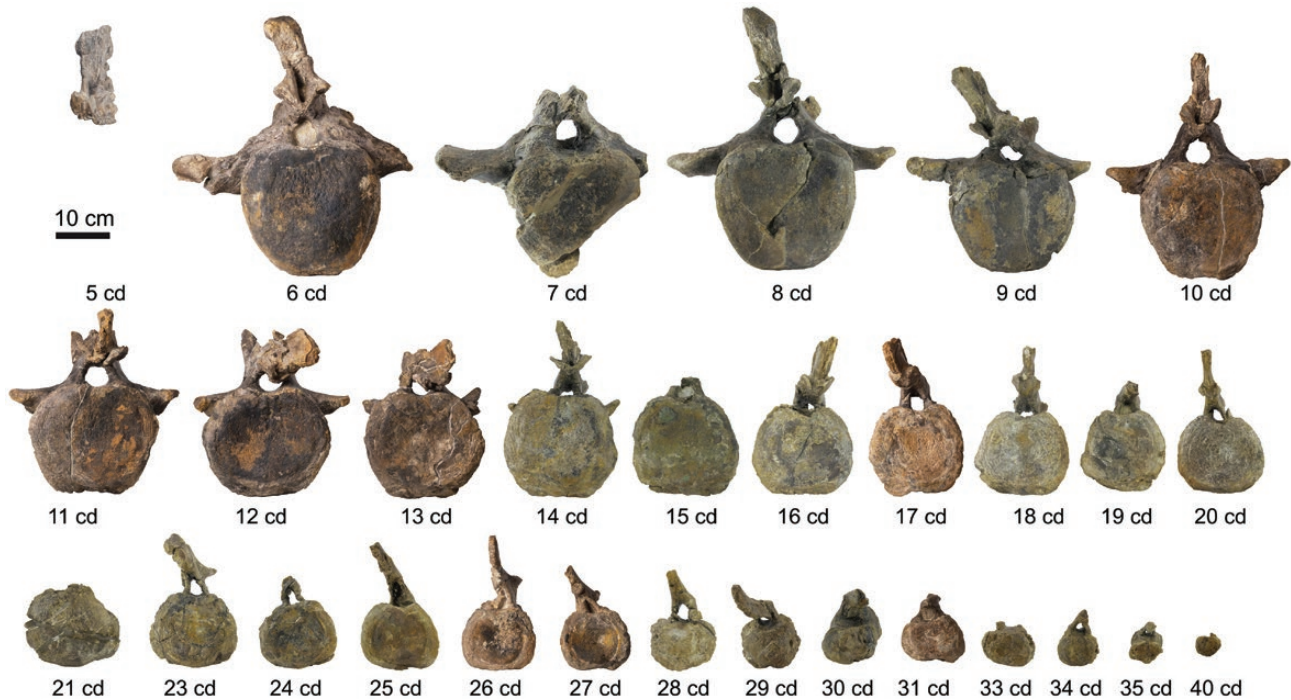


Figure 8. Caudal vertebrae in posterior views of *Losillasaurus giganteus* (San Lorenzo specimen): 4th (MAP-6050), 6th (MAP-6052), 7th (MAP-1846b), 8th (MAP-6053), 9th (MAP-6054), 10th (MAP-6055), 11th (MAP-6056), 12th (MAP-6057), 13th (MAP-6058), 14th (MAP-6059), 15th (MAP-6062), 16th (MAP-6061), 17th (MAP-6060), 18th (MAP-6063), 19th (MAP-6064), 20th (MAP-6066), 21st (MAP-6065), 23rd (MAP-6068), 24th (MAP-6069), 25th (MAP-6070), 26th (MAP-6071), 27th (MAP-6072), 28th (MAP-6073), 29th (MAP-6074), 30th (MAP-6075), 31st (MAP-6076), 33rd (MAP-6078), 34th (MAP-6079), 35th (MAP-6080) and 40th (MAP-6083).

spine is rugose and lacks a transversely constricted and deep prespinal lamina. This is similar to the posterior face, where the surface is also rugose and lacks a postspinal lamina and the spinopostzygapophyseal fossa. The neural spine is larger anteroposteriorly than transversely. One important character is the presence of a rugose ridge at the base of the spine between the prezygapophyses. It is oriented perpendicularly to the spine and does not continue towards the dorsal spine, differentiating it from the prespinal lamina. This ridge is present in the *Losillasaurus* type specimen and in *Turiasaurus* (Puntal de Santa Cruz specimen, RD-13; [Royo-Torres et al., 2009](#)). It is thus considered a possible synapomorphy for Turiasauria. The character is possibly present between the second to ninth caudal vertebrae and disappears from the tenth one onwards. In other sauropods, such as *Tastavinsaurus*, a thin lamina appears in the same position, but in the fossa that exists between the prezygapophyses. Finally, another important feature is the presence of a dorsoventral ridge on the anterolateral surface of the spine from the third to tenth caudal vertebrae ([Figs 9, 10](#)). The character is also evident in the *Losillasaurus* type specimen in the third to fifth caudal vertebrae. The absence in the first two caudal vertebrae can be

related to the pronounced lateral deformation of the neural spine in the first and second caudal vertebrae of the *Losillasaurus* type specimen. This character is missing in the San Lorenzo specimen from the 11th caudal vertebrae onwards. This character is not developed in the specimen from Puntal de Santa Cruz referred to as *Turiasaurus riodevensis* and is considered a new autapomorphy for *Losillasaurus giganteus*. This character is also present in the isolated vertebra (SHN 180) from the Upper Jurassic Praia de Amoreira-Porto Novo Formation in Baleal (Peniche, Portugal) ([Mocho et al., 2017b](#)). The caudal vertebrae of the San Lorenzo specimen lack a hyposphene similar to the *Losillasaurus* type specimen and SHN 180. The postzygapophyses are joined at the base of the neural spine by a horizontal lamina in the anterior caudal vertebrae, but separated from the tenth caudal vertebra onwards ([Fig. 8](#)).

Chevrons

In total, 21 chevrons (MAP-6085 to MAP-6110) have been recovered for this specimen ([Fig. 11](#); [Supporting Information, File S3](#)). They represent the anterior, middle and posterior chevrons in a continuous series,

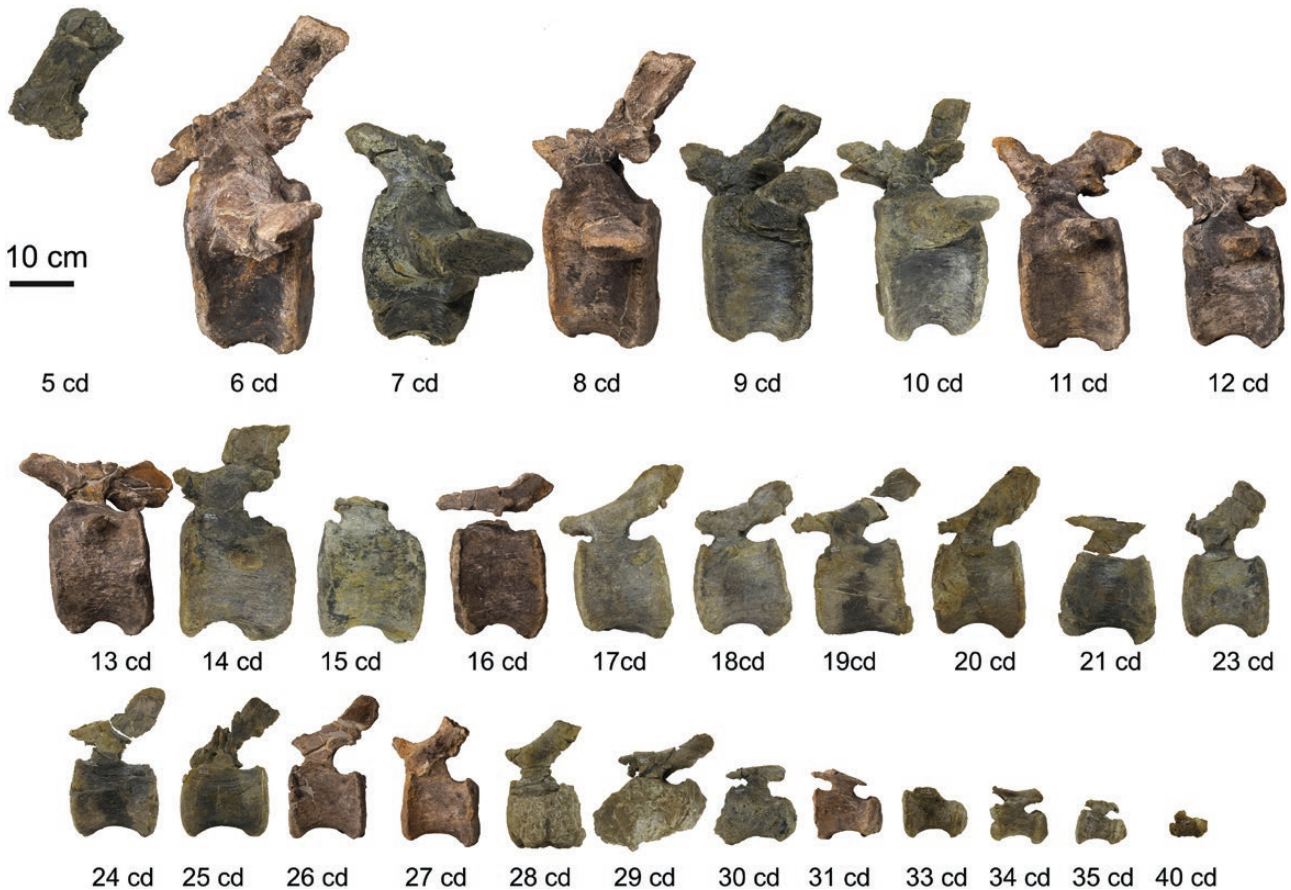


Figure 9. Caudal vertebrae in lateral views of *Losillasaurus giganteus* (San Lorenzo specimen): 5th (MAP-1846a), 6th (MAP-6052), 7th (MAP-1846b), 8th (MAP-6053), 9th (MAP-6054), 10th (MAP-6055), 11th (MAP-6056), 12th (MAP-6057), 13th (MAP-6058), 14th (MAP-6059), 15th (MAP-6062), 16th (MAP-6061), 17th (MAP-6060), 18th (MAP-6063), 19th (MAP-6064), 20th (MAP-6066), 21st (MAP-6065), 23rd (MAP-6068), 24th (MAP-6069), 25th (MAP-6070), 26th (MAP-6071), 27th (MAP-6072), 28th (MAP-6073), 29th (MAP-6074), 30th (MAP-6075), 31st (MAP-6076), 33rd (MAP-6078), 34th (MAP-6079), 35th (MAP-6080) and 40th (MAP-6083).

showing three different morphological types. The first chevron is likely formed by two separated left and right distal blades with an inverted ‘U’-shaped morphology (Serenó *et al.*, 1999). The remaining anterior chevrons display two dorsal rami that are dorsally bridged and ventrally fused. The distal end corresponds to a single blade structure and is ‘Y’-shaped in the anterior and posterior views. The relative length of the main stem of the ‘Y’ gradually shortens until forming a ‘V’ shape while moving backwards along the tail. The third type is represented by a forked structure in the middle and posterior chevrons, such as in non-macronarian eusauropods (Otero *et al.*, 2012). The proximal ends of the anterior and middle chevrons are dorsally bridged by a bar of bone, while the posterior chevrons are dorsally open. This feature is similar in basal neosauropods such as diplodocoids. However, it is different in more derived sauropods like *Mamenchisaurus*, *Omeisaurus*

Young, 1939 or *Tazoudasaurus* Allain *et al.*, 2004, in which all chevrons are closed (Otero *et al.*, 2012). In *Camarasaurus*, the presence of this bridge seems to depend on the ontogeny, as some chevrons are open while others are closed (Ikejiri *et al.*, 2005). The ratio of the dorsoventral length of the haemal canal to the total length of chevron in the first ten anterior chevrons is less than 0.30 (0.27). Thus, this condition is primitive with respect to *Europasaurus* and Titanosauriformes, which have haemal canals representing 50% of the chevron length (Wilson, 2002; D’Emic, 2012). However, the extension of the haemal canal in the San Lorenzo specimen is greater than that of *Mamenchisaurus* (Ouyang & Ye, 2002), *Apatosaurus* (Upchurch *et al.*, 2004b), and deeply nested Titanosauriformes, such as *Tamabatitanis* (Saegusa & Ikeda, 2014). This ratio is 0.40 in the middle chevrons (relative position, 14th) and greater than 0.50 in the posterior ones (relative position, 17th).

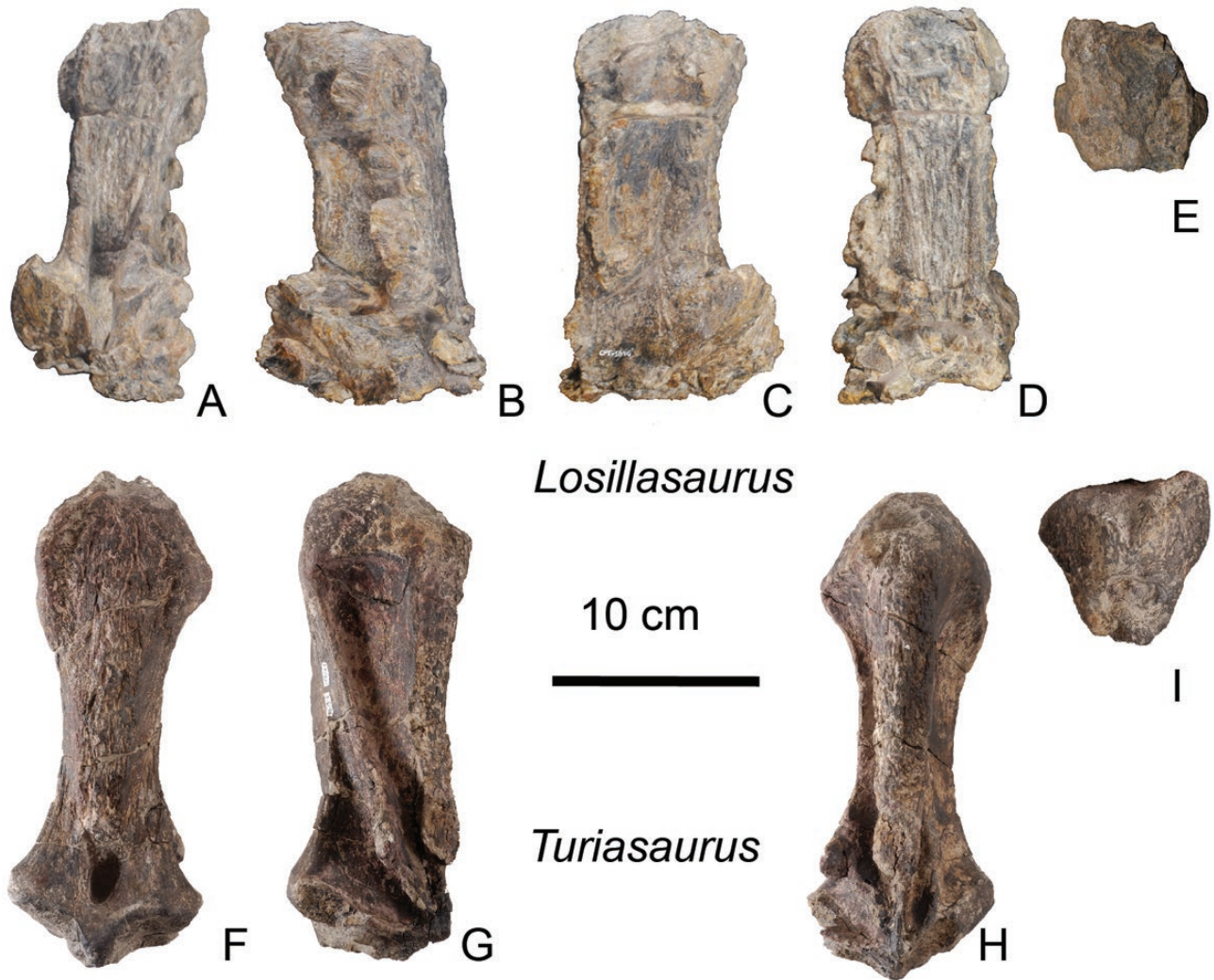


Figure 10. Comparison of the caudal spines of *Losillasaurus giganteus* (CPT-1846, San Lorenzo specimen) in posterior (A), right lateral (B), left lateral (C), anterior (D) and dorsal (E) views and *Turiasaurus riodevensis* (CPT-1611, Puntal de Santa Cruz) in posterior (F), right lateral (G), anterior (H) and dorsal (I) views.

Forelimb

The left ulna (MAP-6111) is the only well-preserved bone from the forelimb. The ulna (Fig. 12; Supporting Information, File S3) is a relatively slender element. In proximal view, the ulna is triradiate, as in every sauropod (McIntosh, 1990; Upchurch *et al.*, 2004a), with the anteromedial process (amp) and anterolateral (alp) processes meeting each other at approximately 90° (Fig. 12). The amp is longer than the alp (ratio = 1.48), which is similar to the condition in most sauropods (see table 2 in Upchurch *et al.*, 2015). The ulna (MAP-6111) differs from the subequal proximal processes seen in *Mamenchisaurus* (Ouyang & Ye, 2002), *Omeisaurus* (He *et al.*, 1988; Läng, 2008), *Shunosaurus* Dong *et al.* 1983 (Läng, 2008) and diplodocoids (Wilson, 2002). The San Lorenzo specimen is different to from some

titanosauriforms, as it has with a long amp (Upchurch *et al.*, 2015; Mannion *et al.*, 2017). The articular surface of the amp process is slightly concave along its length and transversely flat. Both processes define a slightly anterior fossa with dorsoventrally oriented ridges that receives the proximal end of the radius (Fig. 12), as in other eusauropods (Wilson & Sereno, 1998). The olecranon region, where the anteromedial and anterolateral proximal processes meet, is low and shorter than the amp and alp processes. Thus, the *San Lorenzo* specimen possesses the reduced derived olecranon that occurs in other turiasaurs such as *Zby* (Mateus *et al.*, 2014) and *Mierasaurus* (Royo-Torres *et al.*, 2017) and in most sauropods except some titanosaurs, where a more prominent olecranon is reacquired (Upchurch, 1995, 1998; Wilson, 2002).

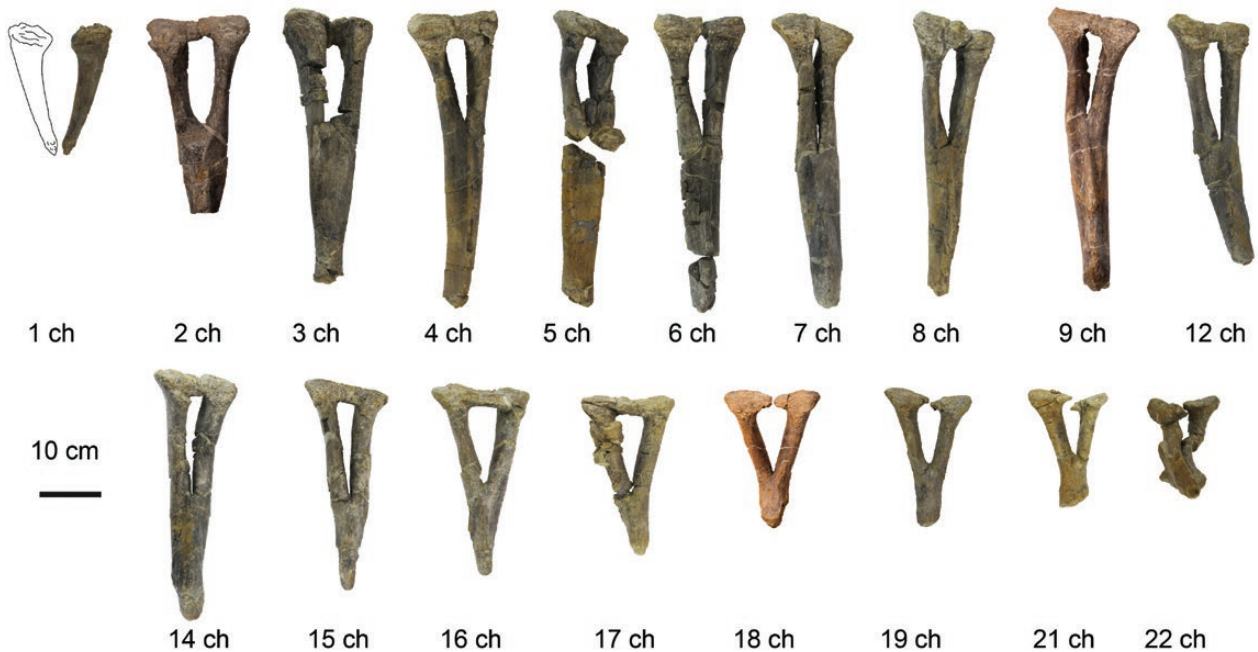


Figure 11. Chevrons of *Losillasaurus giganteus* (San Lorenzo specimen) in posterior view: from anterior to posterior, chevron 1 to chevron 9 (MAP-6085 to MAP-66093), chevron 12 (MAP-6096), chevron 14 to 19 (MAP 6098 to MAP-6103), chevron 21 (MAP 6015) and chevron 22 (MAP-6016).

Passing distally along the shaft of the ulna, the amp and alp processes and radial fossa gradually decrease in prominence, disappearing at around mid-height in a similar way to those in *Turiasaurus* (Royo-Torres *et al.*, 2006) and *Zby* (Mateus *et al.*, 2014). The posterior surface of the proximal half of the ulna is strongly concave mediolaterally (Fig. 12) and bounded by the distal extension of the amp process and a ridge formed along the proximal half of the posterolateral margin. Therefore, this deep fossa rivals the radial fossa in depth. This strong concavity is probably a feature in turiasaurs such as *Losillasaurus*, *Mierasaurus*, *Moabosaurus*, *Turiasaurus* and *Zby* (Royo-Torres *et al.*, 2017). In other sauropods, this concavity is only slightly developed, except in several somphospondylans, where it has also been described (Upchurch *et al.*, 2015). The anterior surface of the distal half of the ulna has a deep vertical groove and ridge as seen in *Turiasaurus* (CPT-1197) and *Losillasaurus* (MCNV). This character was erroneously interpreted as a synapomorphy for Turiasauria (Royo-Torres *et al.*, 2006; but amended in Royo-Torres *et al.*, 2017), as it was interpreted as being present on the posterior surface of the distal half of the ulna. Thus, character number 413 used by Mannion *et al.* (2017, 2019) should be deleted (Royo-Torres *et al.*, 2017). It is codified here with a ‘?’ for each taxa in the phylogenetic analyses. The articular surface of the ulna in *Turiasaurus* is damaged, and the proximal profile of the ulna is shaped between a ‘T’ and ‘Y’.

Femur

The femur of the San Lorenzo specimen (MAP-6113; Fig. 13; Supporting Information, File S3) is straight in all views. An articular head at the proximal end projects dorsomedially in the anterior view. The head is not separated from the greater trochanter by a constriction, a feature usually present in sauropods (McIntosh, 1990; Upchurch *et al.*, 2004a). The head is rounded, subspherical, tapers laterally and is narrow in the greater trochanter. The shaft is oval in cross-section, transversely. In the anterior and posterior views, the section has the same length and tapers slightly in the middle. The femur lacks a ‘lateral bulge’ in its lateral surface in the proximal third, a feature that allows the exclusion of the San Lorenzo specimen from the Titanosauriformes’ clade (Salgado *et al.*, 1997; Wilson & Sereno, 1998). The lateral margin of the proximal end is straight relative to the lateral margin of the midshaft and lacks a medially deflected lateral margin (Royo-Torres *et al.*, 2012; Mannion *et al.*, 2013), which is similar to the case of non-macronarian eusauropods. The fourth trochanter is located on the posteromedial margin of the shaft at midlength, where it is reduced to a low ridge. The distal end is divided into two condyles: the tibial condyle is twice as big as the fibular one. This condition is different in other turiasaurs, such as *Mierasaurus* (DBGI 39), and could be an autapomorphy. Usually, the tibial condyle is larger than the fibular one in all sauropods,

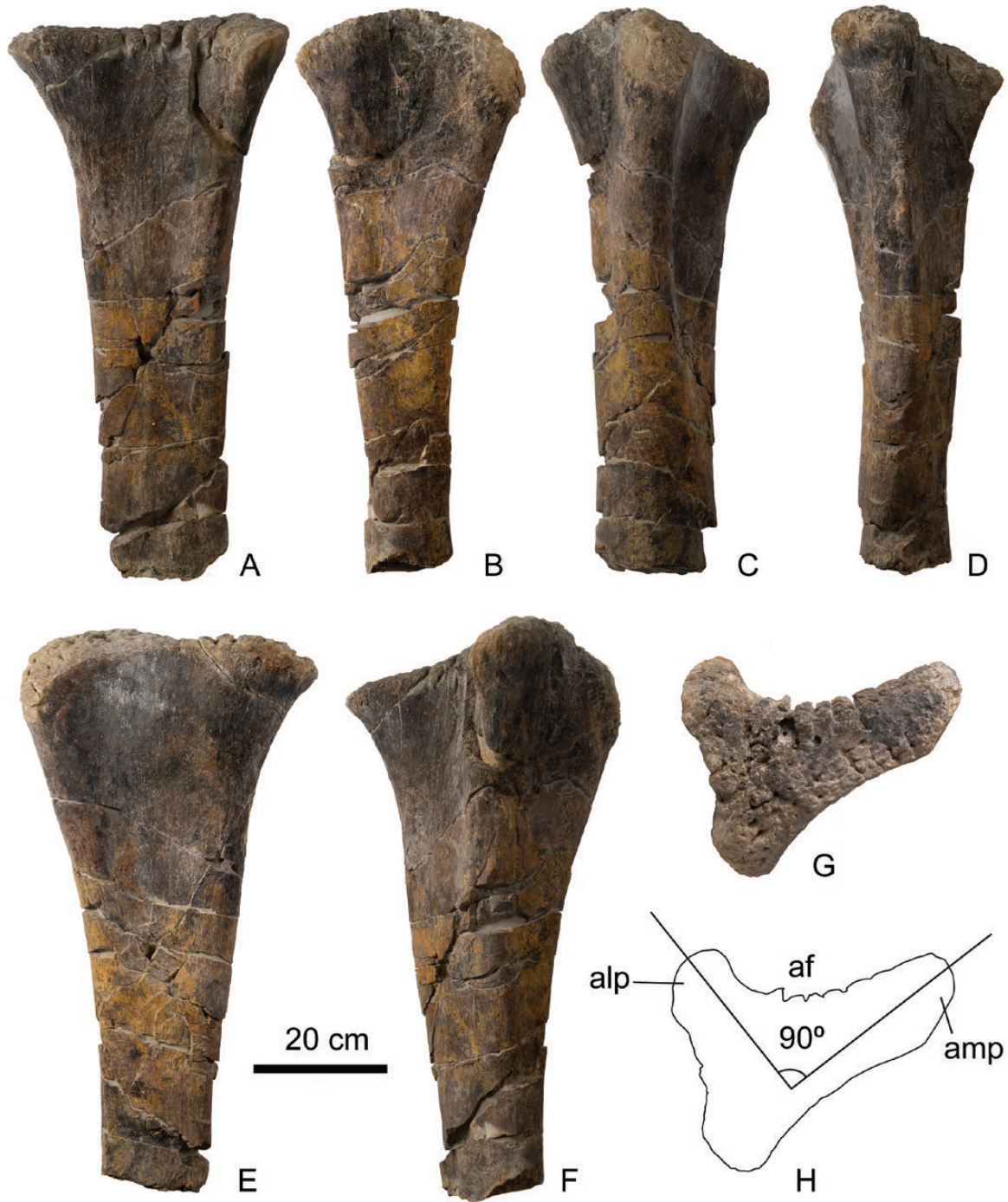


Figure 12. Left ulna (MAP-6111) of *Losillasaurus giganteus* (San Lorenzo specimen) in anterior (A), lateral (B), posterior (C), anteromedial (D), medial (E), anterolateral (F) and dorsal (G, H) views.

such as *Brachiosaurus* Riggs, 1903 and *Giraffatitan* (HMN St 291, Janensch, 1961), but smaller than in the San Lorenzo specimen. In the posterior margin there is a notch lateral to the fibular condyle, as is usual in most dinosaurs (Upchurch, 1995, 1998). The

intercondylar groove is shallow on the distal part of the anterior face. However, the tibial and fibular condyles display a deep intercondylar groove on their posterior faces. The articular condyles are rotated so that their long-axes are directed anterolaterally at an



Figure 13. Right femur (MAP-6113) of *Losillasaurus giganteus* (San Lorenzo specimen) in dorsal (A), ventral (B), medial (C), posterior (D), lateral (E) and anterior (F) views.

angle of approximately 20° to the parasagittal plane, as also occurs in *Apatosaurus* (Upchurch *et al.*, 2004b) whose long axis of the transverse section of the shaft is horizontal.

Tibia

The tibia (MAP-6115; Fig. 14; Supporting Information, File S3) is straight. The tibia to femur length ratio is 0.65 and, therefore, within the typical range of those in sauropods (McIntosh, 1990; Upchurch *et al.*, 2004a). The proximal articular surface is between subcircular and transversely compressed, a plesiomorphic condition for Sauropoda (Wilson, 2002; Tschopp *et al.*, 2015). The anterolateral corner of the proximal end displays a rounded triangular cnemial process, which is an anteriorly projecting and vertically elongate ridge. The lateral margin of the proximal end bulges laterally, forming a vertical groove between its anterior face and posterior face of the cnemial crest. A small ridge posterior to the cnemial crest is present at the top of this groove. This crest is interpreted as the second cnemial crest described by Bonaparte *et al.* (2000) for the tibia (SMNS 12144) of *Janenschia*. In the San Lorenzo specimen, this crest is markedly pointed and parallel to the cnemial crest. This feature is present in

most eusauropods, but absent in most diplodocoids and somphospondylans (Mannion *et al.*, 2013). The area for the ‘tuberculum fibularis’ is rugose and there is a small vertical ridge, different to the ridge in the tibia of *Suuwassea* Harris & Dodson, 2004 (Harris, 2007). The distal end is less expanded than the proximal end and has a rough surface with a heart-shaped outline in the ventral view. Both malleoli are laterally oriented, and the anterior one is larger and square in shape. It also displays the articular surface for the ascending process. The posterior malleolus is smaller and rounded. It is described as a posterior ventral process. The posterior condyle projects more distally and meets the posterior side of the ascending process of the astragalus. The ratio between the mediolateral and anteroposterior widths is close to 1.

Fibula

The fibula (MAP-6116; Fig. 15; Supporting Information, File S3) is a straight bone with an expanded proximal end. The distal end is not preserved. The proximal end of the fibula is anteroposteriorly elongated and transversely flattened and rectangular in the dorsal view. The lateral surface is convex and the medial one concave.



Figure 14. Right tibia (MAP-6115) of *Losillasaurus giganteus* (San Lorenzo specimen) in dorsal (A), ventral (B), medial (C), posterior (D), anterior (E) and lateral (F) views.

The latter surface displays a triangular muscle scar. The anterior margin has a sharp triangular expansion in the lateral and medial views with a medially oriented vertical ridge. The proximal end is twice the anteroposterior length of the diaphysis, differentiating it from that in *Turiasaurus* and *Camarasaurus*. The lateral trochanter is a concave surface, different to the flat and rugose surface present in *Turiasaurus*. The lateral muscle insertion scar shares the plesiomorphic oval shape of those in *Omeisaurus* and *Shunosaurus*. This shape is different from that in a trochanter associated with one or two vertical elongate ridges, as occurs in some Titanosauriformes (D’Emic, 2012; Mannion *et al.*, 2019).

Astragalus

The astragalus (left: MAP-6117; right: MA-6118) is wider transversely than anteroposteriorly (Fig. 16; Supporting Information, File S3), typical of Sauropoda (McIntosh, 1990; Upchurch *et al.*, 2004a). Its lateral end is broad and tapers medially to a blunt point, but is more rounded than in the case of *Turiasaurus* (Fig. 16). The ventral surface is rugose and convex, both anteroposteriorly and transversely. The ascending process is flat and runs two-thirds of the

posterior margin of the main body of the astragalus. The astragalus is wedge-shaped in proximal view and becomes medially narrow in anterior view. The anterior edge is straight-to-convex transversely in the proximal view. Laterally, there is a ventral shelf underlying the distal end of the fibula. The lateral surface of the astragalus has a central concavity, which is not deflected posteriorly. The posterior astragal fossa is deep and bears two main foramina separated by a subvertical ridge, as in *Lapparentosaurus* Bonaparte, 1986 (Läng, 2008) and *Oceanotitan* Mocho *et al.*, 2019. This subvertical ridge is another important difference from the astragalus of *Turiasaurus* (Fig. 16). The posterodistal edge of the astragalus, ventral to the ascending process, is laterally projected, resulting in a pronounced and flat tongue-like structure. The laterally facing articular surface for the fibula is concave, well-marked and occupies the dorsal part of the lateral surface of the astragalus.

TAXONOMIC ASSIGNATION OF THE SAN LORENZO SPECIMEN

Following the description of the San Lorenzo specimen, it is considered to possess characters that differ from *Turiasaurus*, *Zby* and others that have



Figure 15. Right fibula (MAP-6116) of *Losillasaurus giganteus* (San Lorenzo specimen) in medial (A), dorsal (B), anterior (C), lateral (D) and posterior (E) views.

only been previously described in *Losillasaurus*. Some are new and must be included in a revised diagnosis (see below) for this genus. Both the *Losillasaurus* type and San Lorenzo specimen share the following new autapomorphies, which are not present in any other sauropod: the presence of a dorsoventral ridge in the anterolateral surface of the spine at least between the fourth and tenth caudal vertebrae. This character has been confirmed as absent in the *Turiasaurus* specimen from the Puntal de Santa Cruz site (Royo-Torres *et al.*, 2009), in which an anterior caudal spine (CPT-1649) has been identified (Fig. 10). Another character seen in the *Losillasaurus* holotype and San Lorenzo specimen is a spine with a shallow dorsal groove projected anteroposteriorly. This groove is bigger in the anterior caudal vertebrae, especially in the first and second caudal vertebrae (*Losillasaurus* type specimen) and then shallow from the third to 30th caudal vertebrae (*Losillasaurus* type and San Lorenzo specimens). Based on the anatomical descriptions and comparisons, it is concluded that the San Lorenzo specimen should be classified as *Losillasaurus giganteus*, a hypothesis also supported by the phylogenetic analyses performed (see below and Supporting Information, File S1).

PHYLOGENETIC ANALYSES

We performed the analyses using extended implied weighting (Goloboff, 2014), with the default settings in TNT. The pruned data matrix was analysed using the Search in TNT v.1.5 (Goloboff *et al.*, 2008; Goloboff & Catalano, 2016). Searches were conducted by employing sectorial searches, drift and tree fusing. Consensus was stabilized five times before using the resultant trees as the starting trees for a 'Traditional Search' using Tree Bisection-Reconstruction. The first analysis includes the San Lorenzo specimen as separated OTU from *Losillasaurus* type and the new taxa from the Middle Jurassic of Madagascar (119 OTUs). This produced 135 MPTs with a length of 239.99 steps and a well-resolved strict consensus (Supporting Information, File S1, Fig. S1). The San Lorenzo specimen and *Losillasaurus* type are sister-taxa of *Turiasaurus*. They are all recovered as members of the Turiasauria clade and the new taxa from the Middle Jurassic of Madagascar is given as a sister-taxon of European turiasaurs. We ran another analysis, which positioned the *Losillasaurus* type and San Lorenzo specimen in the same OTU (118 OTUs). The result (Fig. 18) is similar to the previous analysis and produced 135 MPTs with a 239.7 step length. We also performed the analyses using conventional equal

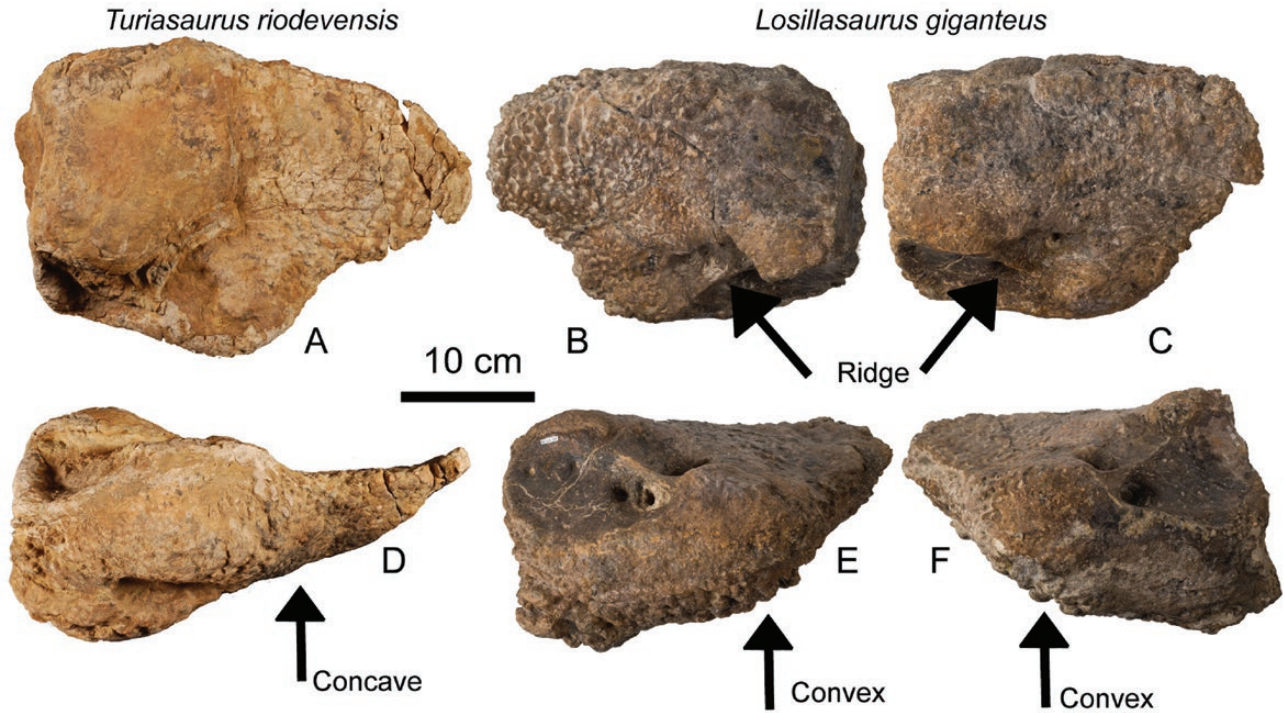


Figure 16. Comparison between astragali. Left astragalus (CPT-1244) in dorsal (A) and posterior (D) views of *Turiasaurus riodevensis* (paratype) and right (B, E) (MAP-6119) and left (C, F) astragalus (MAP-6117) of *Losillasaurus giganteus* (San Lorenzo specimen) in dorsal (B, C) and posterior (E, F) views.

weights parsimony (Goloboff, 2014). The results of the analysis with 99 999 MPTs (overflow) and 2591 step length show a polytomy for Eusauropoda (Supporting Information, File S1, Fig. S2).

SYSTEMATIC PALAEOLOGY

SAUROPODA MARSH, 1878

EUSAUROPODA UPCHURCH, 1995

TURIASAURIA ROYO-TORRES *ET AL.*, 2006

LOSILLASAURUS CASANOVAS *ET AL.*, 2001

Figures: See Casanovas *et al.*, 2001: figs 1–7; Figs 1–16; Supporting Information, File S3.

Type species: *Losillasaurus giganteus* Casanovas *et al.* (2001).

Holotype: Anterior caudal vertebra housed in the Museo de Ciencias Naturales de Valencia (MCNV).

Paratype: Two anterior caudal vertebrae housed in the Museo de Ciencias Naturales de Valencia (MCNV).

Type locality and horizon: La Cañada site (Valencia), Villar del Arzobispo Formation (Casanovas

et al., 2001; Royo-Torres *et al.*, 2006). Dated as Kimmeridgian according to the data of Campos-Soto *et al.* (2019).

Referred material: The material referred to *Losillasaurus* comes from the same specimen from where the holotype and paratype were selected. It consists of a skull fragment and partial postcranial skeleton (see Supporting Information, File S1). A second specimen, described in this paper, is from the San Lorenzo site (Riodeva, Teruel, Spain) in the Villar del Arzobispo Formation. It consists of a partial skull with teeth and partial postcranial skeleton (see the previous description section and Supporting Information, File S1). A third specimen referred to as *Losillasaurus* is a complete anterior caudal vertebra (SHN 180) found in Baleal (Peniche municipality, Portugal) in the Praia de Amoreira-Porto Novo Formation, dated as Upper Kimmeridgian–Lower Tithonian (Manuppella *et al.*, 1999; Mocho *et al.*, 2017b).

Revised diagnosis: *Losillasaurus* is diagnosed by eight autapomorphies: (1) (new) lateral surface of the premaxilla and maxilla with dorsoventrally elongated grooves convergent with diplodocids and *Nemegtosaurus* (Mannion *et al.*, 2019); (2) (new) a maxillary tooth with a secondary apex on the distal

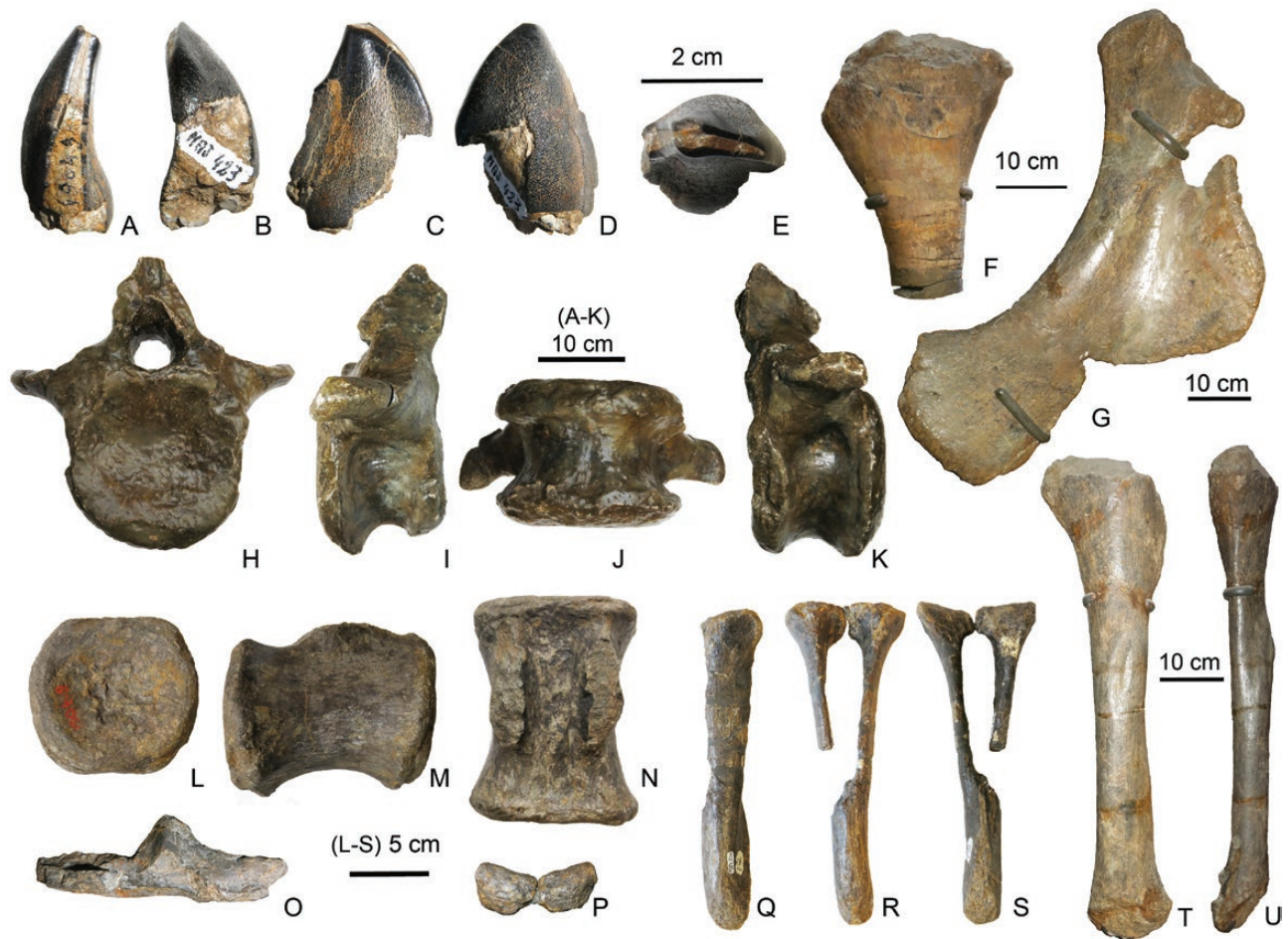


Figure 17. *Narindasaurus thevenini*: right premaxillary-maxillary teeth (MNHN MAJ 423) in mesial (A), distal (B), lingual (C), labial (D) and apical (E) views; right tibia (MNHN MAJ 428) in medial view (F); left pubis (MNHN MAJ 430) in lateral view (G); anterior caudal vertebrae (MNHN MAJ 424) in anterior (H), right lateral (I), ventral (J) and left lateral (K) views; posterior caudal vertebrae (MNHN MAJ 426) in posterior (L), right lateral (M) and dorsal (N) views; distal chevron (MNHN MAJ 429) in right lateral view (O); middle-anterior chevron (MNHN MAJ 425) in dorsal (P), right lateral (Q), posterior (R) and anterior (S) views; and right fibula in lateral (T) and anterior (U) views from the same specimen.

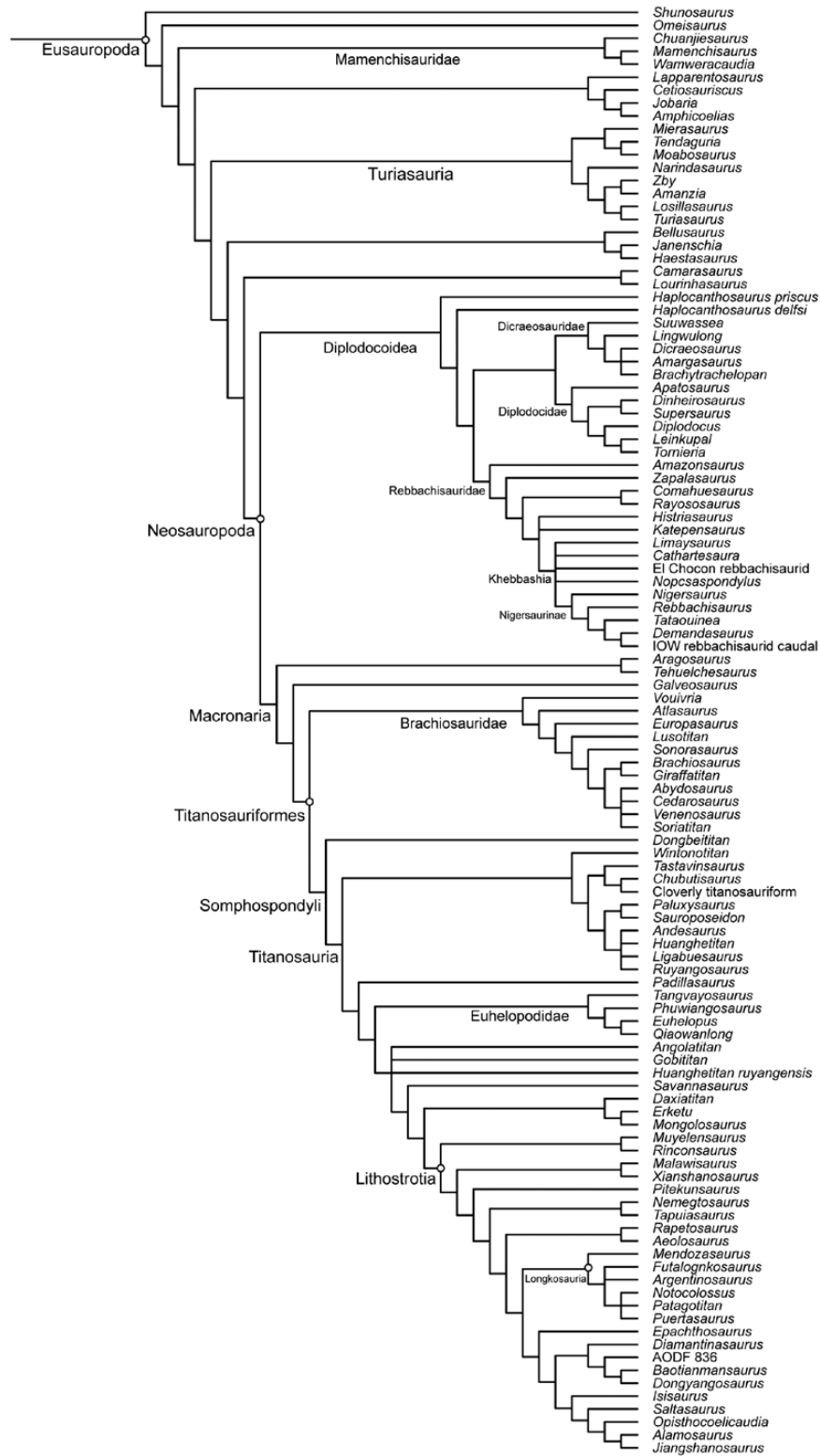
edge; (3) markedly curved neural spines of the proximal caudal vertebrae that in the first and second caudal vertebrae produce a pronounced cutlass-like shape in the lateral view (Casanovas *et al.*, 2001; Upchurch *et al.*, 2004a); (4) (new) presence of a dorsoventral ridge in the anterolateral surface of the spine at least between the fourth and tenth caudal vertebrae (it is not clearly present in the first three caudal vertebrae and disappears in the 11th caudal vertebra); (5) (new) caudal neural spines with a shallow dorsal groove with directed anteroposteriorly, bigger in the anteriormost caudal vertebrae, especially in the first and second bones and shallow from the third to the 30th caudal vertebrae; (6) (new) the long-axis of the obturator foramen is perpendicular to the long-axis of the pubis; (7) (new) the lateral trochanter of the fibula is concave and rugose; and (8) (new) the tibial

condyle of the femur is twice as large as the fibula condyle.

Additional comments: The character, anteroposterior length at the base of the neural spines of the proximal caudal vertebrae being approximately half the height of the spine (ratio = 0.5), was included in the original diagnosis (Casanovas *et al.*, 2001) and accepted in Upchurch *et al.* (2004a). However, this is not considered valid as the spines are compressed by taphonomic deformation.

NARINDASAUROS THEVENINI GEN. & SP. NOV.

Figures: See Thevenin (1907): pl. 1, figs 1, 1a–1c, 6–6a, 7–7a, 9, 9a.; pl. 2, figs 5–8; Lång (2008): figs II-24,



Downloaded from https://academic.oup.com/zoolinnean/advance-article/doi/10.1093/zoolinnean/zlaa091/5900936 by guest on 05 September 2020

Figure 18. Strict consensus cladogram of extended implied weight analysis (with the same protocol as Mannion *et al.*, 2019) with *Losillasaurus giganteus* coded with the holotype, paratype and the referred to San Lorenzo specimen together and new taxon *Narindasaurus thevenini*.

II-25, II-26, II-27, II-28; Mannion (2010): figs 4a–d, 17; Supporting Information, File S4.

Zoobank: Genus: [Urn:lsid:zoobank.org:act:B7203900-1F11-40CD-B4D5-115BAD1B96FE](https://zoobank.org/urn:lsid:zoobank.org:act:B7203900-1F11-40CD-B4D5-115BAD1B96FE); species: [Urn:lsid:zoobank.org:act:E3ED87DE-59E2-428C-B26E-0BBBFD38272B](https://zoobank.org/urn:lsid:zoobank.org:act:E3ED87DE-59E2-428C-B26E-0BBBFD38272B):

Etymology: The genus is named for Narinda Bay, close to the Ankinganivalaka site where the type specimen was found, and from Ancient Greek σαῦρος (*saûros*), lizard. The species name honours Armand Thevenin, French palaeontologist who was interested in the Jurassic dinosaurs of Madagascar at the beginning of the 20th century. He published the first elements of this sauropod in 1907.

Holotype: A partial skeleton composed by a right maxillary or premaxillary tooth (MNHN MAJ 423), an anterior caudal vertebra (MNHN MAJ 424), posterior caudal vertebra (MNHN MAJ 426), middle-anterior chevron (MNHN MAJ 425), right ulna (MNHN MAJ 427), right tibia (MNHN MAJ 428), right fibula with a distal chevron attached (MNHN MAJ 429) and left pubis (MNHN MAJ 430). All elements belong to the same individual (Läng, 2008). They are deposited at the Muséum national d'Histoire naturelle (Paris, France).

Type locality and horizon: Ankinganivalaka municipality (previously known as Ankingavola), on the right bank of a meander of the Loza River in the middle part of the Isalo III Formation (Bathonian, Middle Jurassic) (Lemoine, 1906; Besairie & Collignon, 1972; Läng, 2008).

Diagnosis: It can be diagnosed by one autapomorphy (marked with an asterisk), as well as a unique combination of derived diagnostic characters: (1) middle-anterior caudal vertebrae with an asymmetric lateral fossa set in a posterior position (*); (2) longitudinal ridge on the lateral face of the pubis, from the anterior area of the obturator foramen to its distal end; (3) perpendicular angle between the ischial articulation and posterior pubic symphysis of the pubis; (4) the distal end of the pubis presents an obtuse angle between the ventral and anterior surfaces in the lateral and medial views; and (5) outwardly developed triangular lateral trochanter of the fibula, which is visible in the anterior and posterior views.

Additional comments: This taxon was first diagnosed by Thevenin (1907) as part of the genus '*Bothriospondylus*'. However, a more modern study (Mannion, 2010) considered this genus invalid.

Läng (2008) and Mannion (2010) interpreted the Ankinganivalaka material as belonging to a non-neosauropod eusauropod taxon. Furthermore, Mocho *et al.* (2016) classified the teeth of this specimen as the typical heart-shaped teeth of the Turiasauria clade. A complete description of this sauropod was provided by Läng (2008) and Mannion (2010).

DISCUSSION

DISCUSSION OF HOLOTYPE MATERIAL OF *NARINDASAURUS THEVENINI*

Here, we compare *Narindasaurus thevenini* with taxa possessing similar features from the similar Middle Jurassic age, finding that it differs from all of the considered taxa. For example, *Lapparentosaurus* lacks a long ridge in the lateral face of the pubis and has a block-shaped hyposphene in the anterior caudal vertebrae and an ambiens process in the proximal part of the pubis. Both these features are absent in the material of *Narindasaurus thevenini*. Other Middle Jurassic taxa from Africa are also different: the teeth of *Chebsaurus* Mahammed *et al.*, 2005 lack the lingual apicobasal ridge typical of the turiasaur taxa. This feature is present in the teeth of *Narindasaurus thevenini*. In addition, *Chebsaurus* has dorsally open chevrons (Läng & Mahammed, 2010), while in *Narindasaurus thevenini*, they are dorsally bridged (Thevenin, 1907). Another genus from the Middle Jurassic of Madagascar is *Archaeodontosaurus Buffetaut*, 2005, which also has different teeth (Mannion, 2010) and lacks the heart-shaped ones of *Narindasaurus*. Some characters, such as the lateral trochanter of the fibula developed outwards and the lateral ridge in the pubi, are described in some titanosaurs of the Late Cretaceous (Mannion *et al.*, 2019). For example, the character of the pubis is shared with *Uberabatitan* Salgado & Carvalho, 2008 and the character of the fibula is shared with some titanosaurs, such as *Bonitasaura* Apesteguía, 2004 (Gallina & Otero, 2015), *Laplataosaurus* Huene, 1929 and *Neuquensaurus* Powell, 1992 (Otero, 2010). The lateral fossa in the caudal vertebrae is described in some titanosauriforms, but is not asymmetrical and posteriorly located, as in *Narindasaurus thevenini*. In the Ankinganivalaka specimen, the fossa is anteriorly pointed and expands posteriorly, while in *Cedarosaurus* Tidwell *et al.*, 1999 and *Venosaurus* Tidwell *et al.*, 2001 it is elliptical in shape (Tidwell *et al.*, 1999, 2001). *Narindasaurus thevenini* shares the heart-shaped-tooth diagnostic character with the Turiasauria clade and, according to the phylogenetic analysis (see below), *Narindasaurus thevenini* is a member of the Turiasauria clade. This specimen is

of high systematic importance, because it presents a combination of characters not typical in any known sauropod (Läng, 2008; Mannion, 2010). In the current work, we codify this specimen for the first time in a morphological dataset to conduct a phylogenetic analysis (see below). The results locate it at the base of the European Turiasauria clade.

DISCUSSION OF THE PHYLOGENETIC RESULTS

The first analysis includes *Narindasaurus* and resulted in a well-resolved strict consensus (Supporting Information, File S1, Fig. S1). The San Lorenzo specimen and *Losillasaurus* type are sister-taxa of *Turiasaurus*. They are all recovered as members of the Turiasauria clade. *Narindasaurus thevenini* is given as a sister-taxon of European turiasaurs and *Moabosaurus*, *Mierasaurus* and *Tendaguria* appear in another turiasaur clade (sister-clade of the European turiasaurs and *Narindasaurus*).

We ran another analysis, which positioned the *Losillasaurus*-type and San Lorenzo specimen in the same OTU (118 OTUs). We have two possible groups of turiasaurs: one for *Narindasaurus* as a sister-taxon of the European turiasaurs during the Jurassic, with *Amanzia*, *Losillasaurus*, *Turiasaurus* and *Zby*, and another clade for the Late Jurassic and Early Cretaceous turiasaurs from Africa and North America. The latter clade includes *Tendaguria* with *Moabosaurus* and *Mierasaurus* as a second family of turiasaurs, which might imply the recovery of the Tendaguriidae clade established by Bonaparte *et al.* (2000). However, we prefer to wait until the relationships are tested with new data and further analyses, as suggested by Mannion *et al.* (2019). The analyses using conventional equal-weight parsimony (Goloboff, 2014) show a polytomy for Eusauropoda (Supporting Information, File S1, Fig. S2). The clade of Turiasauria appears with the African taxa (*Tendaguria*), the American taxa (*Mierasaurus* and *Moabosaurus*) and the European taxa (*Losillasaurus*, *Turiasaurus* and *Zby*). *Amanzia* and *Narindasaurus* are placed outside of Turiasauria. But these results must be looked with caution as the analysis with 99 999 MPTs produced an overflow and there is a general polytomy for Eusauropoda (Supporting Information, File S1, Fig. S2).

SYNAPOMORPHIES OF TURIASAURIA

The present review of the teeth of turiasaurs based on a direct comparison helps us to propose several potential synapomorphies for this clade. Two diagnostic features are identified in the teeth. The first character is that members of Turiasauria possess heart-shaped teeth in the labial and lingual profile with their apex labiolingually compressed, and with

an asymmetrical shape produced by a concave distal margin near the apex, even when unworn (Royo-Torres *et al.*, 2006; Royo-Torres & Upchurch, 2012; Mocho *et al.*, 2016). The second character is the presence of apicobasal low grooves in the root of the teeth (Fig. 5). This character has been seen in *Losillasaurus*, *Moabosaurus* and *Turiasaurus* and in other isolated heart-shaped teeth included as a possible Turiasauria *indet.* This character seems absent in other sauropods such as *Bellusaurus* Dong, 1990 (Moore *et al.*, 2018), *Chebsaurus* (Läng, 2008), diplodocoids such as *Lingwulong* Xu *et al.*, 2018 and *Lavocatisaurus* Canudo *et al.*, 2018 (personal observation RRT & AC, 2018), macronarians such as *Camarasaurus* (Wiersma & Sander, 2017), brachiosaurids such as *Giraffatitan* (personal observation RRT & AC, 2008) and *Vouivria* Mannion, Allain & Moine, 2017, and the titanosaur *Tapuiasaurus* Zaher *et al.*, 2011.

Heart-shaped teeth are known in Middle and Late Jurassic taxa (*Losillasaurus*, *Narindasaurus*, *Turiasaurus* and *Zby*) and in Early Cretaceous taxa (*Mierasaurus* and *Moabosaurus*). The teeth of *Losillasaurus* described in this work demonstrate the heterodonty described in other taxa, such as *Mierasaurus* (Royo-Torres *et al.*, 2017) and suggested in *Turiasaurus* (Royo-Torres & Upchurch, 2012). This result demonstrates that the identified morphological variability is a sample of several Turiasauria-like teeth from the Late Jurassic of Portugal (Mocho *et al.*, 2016). The presence of long longitudinal grooves in the roots is also diagnostic of Turiasauria, which, in the case of *Moabosaurus*, extend to the crown (Britt *et al.*, 2017). In this way, we can identify teeth with both features from the Middle Jurassic, such as the teeth NHMUK R3377 assigned to '*Cetiosauriscus*' from Peterborough (England) (Martill, 1988; Barrett, 2006) and included as possible Turiasauria *indet.* by Royo-Torres and Upchurch (2012) and Mocho *et al.* (2016). Besides the teeth of *Narindasaurus*, two more teeth from Africa are classified as having heart-shaped morphology (Mocho *et al.*, 2016). The first is a tooth (MNHN.F1961-28) from In-Gall (Niger) (Lapparent, 1960), which has a heart-shaped morphology (Mocho *et al.*, 2016). It was found in Irhazer Group sediments and is probably not younger than the Late Middle Jurassic (Rauhut & López-Arbarelló, 2009). The second tooth (UT-TEN15) came from the Tendimirah Quarry, Cabao Formation (Hauterivian–Barremian) in Libya (Le Loeuff *et al.*, 2010). It has a basal constriction and crown similar to the anterior dentary teeth of *Losillasaurus*. It lacks the complex cingulum with associated lingual facets present in *Camarasaurus* and *Euhelopus* Wiman, 1929 (Ostrom & McIntosh, 1966; Wilson & Upchurch, 2009). Finally, the teeth described by Holwerda *et al.* (2015) from Argentina (MPEF-PV-3174 and 3176; see: Holwerda *et al.*,

2015: fig. 2k, l) show a heart-shaped crown and long longitudinal grooves on the root (personal observation, RRT & AC, 2019). These fossils from the El Bagual site suggest the presence of a turiasaur taxon in the Middle Jurassic of South America. This agrees with some phylogenetic analyses carried out by Mannion *et al.* (2019), which recovered *Tehuelchesaurus* Rich *et al.*, 1999 as a form closely related to the Turiasauria clade. However, this result is not supported by our analysis and furthermore, *Tehuelchesaurus* lacks the diagnostic characters for Turiasauria proposed in this work. The European origin of Turiasauria during the Middle Jurassic was also hypothesized when considering the teeth of *Cardiodon* Owen, 1841, '*Cetiosauriscus leedsi*' Hulke (1887) of Peterborough and from Aylesbury (UK) (Royo-Torres & Upchurch, 2012). Currently, the teeth of turiasaurs provide us with more detailed information about the origin and dispersion of this group, which might have occurred during the Middle Jurassic, as predicted by phylogenetic hypotheses (Xu *et al.*, 2018; Mannion *et al.*, 2019).

Turiasauria is also potentially characterized by the following set of synapomorphies in the postcranial elements: (1) (new) the presence of a rugose ridge at the base of the neural spine of the caudal vertebra setting between the prezygapophyses; (2) a medial deflection of the humeral proximal end (Royo-Torres *et al.*, 2006); (3) pronounced bulge on the posterior face of the humeral proximal end (Mateus *et al.*, 2014); (4) dorsoventrally restricted and pronounced deltopectoral crest (Royo-Torres *et al.*, 2006); (5) distal condyles exposed on the anterior face of the humeral distal end (Royo-Torres *et al.*, 2006); (6) posterior face of the humeral distal end being deeply concave transversely (Upchurch *et al.*, 2004a; Mannion *et al.*, 2013); (7) extremely anteroposteriorly compressed proximal end of the radius (Royo-Torres *et al.*, 2006); and (8) the posterior surface of the proximal half of the ulna being strongly concave mediolaterally (Upchurch *et al.*, 2015).

CONCLUSIONS

A new giant specimen of Turiasauria from the Kimmeridgian–Tithonian Villar del Arzobispo Formation in Riodeva (Teruel, Spain) has been described and referred to as *Losillasaurus giganteus*. This specimen helps us to understand tooth variation, allows the positioning of isolated heart-shaped teeth in the skull and demonstrates heterodonty with four morphotypes in Turiasauria. A new diagnosis for *Losillasaurus giganteus* is proposed with eight diagnostic characters. The Turiasauria clade is now characterized by several synapomorphies, including heart-shaped teeth with grooves in the roots. The revision of old Ankinganivalaka

material from the Bathonian Isalo III Formation of Madagascar (Africa) enables us to define a new genus and species: *Narindasaurus thevenini*, which according to the performed phylogenetic analyses, represents the most primitive turiasaur. Thus, the diversity of Turiasauria is extended from the Middle Jurassic to Early Cretaceous, with at least eight probably valid genera recorded, confirming the hypothesis previously predicted by phylogenetic analyses.

ACKNOWLEDGEMENTS

This work was funded by the Departamento de Educación, Cultura y Deporte (Gobierno de Aragón), the Research Group E04_20R FOCONTUR financed by Departamento de Ciencia, Universidad y Sociedad del Conocimiento (Gobierno de Aragón) and FEDER funds 'Construyendo Europa desde Aragón', the Instituto Aragonés de Fomento, Dinópolis. The project PGC2018-094034-B-C22 of the Ministerio de Ciencia, Innovación y Universidades (Gobierno de España). FCT/MCTES for a CEEC Individual contract (CEECIND/00726/2017) and the Synthesys Project, financed by the European Community Research Infrastructure Action under the FP7 (FR-TAF-5072 and DE-TAF-6138). The support of the Willi Henning Society allows TNT to be downloaded free of charge. We thank the following persons for allowing access to specimens in their care: R. Allain (MNHN, France), M. Belinchón (MCNV, Spain), B. B. Britt and R. D. Scheetz (BYU, USA), J. L. Carballido and D. Pol (MPEF, Argentina), R. Castaninha and C. Tomás (ML, Portugal), S. Chapman (NHMUK, UK), D. D. Deblieux and J. Kirkland (UGS, USA), E. Espílez (MAP, Spain), D. Schwarz (HNH, Germany) and B. C. Silva (SHN, Portugal). Ciaran Rowe (Hibernia Idiomas S.L.) edited the text in English, and Taylor & Francis Editing Services revised the final version. The authors thank the anonymous reviewer and associate editor for their help in improving the paper.

REFERENCES

- Barrett PM. 2006. A sauropod dinosaur tooth from the Middle Jurassic of Skye, Scotland. *Transactions of the Royal Society of Edinburgh: Earth Sciences* **97**: 25–29.
- Besairie H, Collignon M. 1972. Géologie de Madagascar, 1. Les terrains sédimentaires. *Annales Géologiques de Madagascar* **35**: 1–463.
- Bonaparte JF, Heinrich WD, Wild R. 2000. Review of *Janenschia* Wild with the description of a new sauropod from the Tendaguru beds of Tanzania and a discussion on the systematic value of procoelous caudal vertebrae in the Sauropoda. *Palaeontographica Abteilung A* **256**: 25–76.

- Britt BB, Scheetz RD, Whiting MF, Wilhite DR. 2017.** *Moabosaurus utahensis*, n. gen., n. sp., a new sauropod from the Early Cretaceous (Aptian) of North America. *Contributions from the Museum of Paleontology, University of Michigan* **32**: 189–243.
- Buffetaut E. 2005.** A new sauropod dinosaur with prosauropod-like teeth from the Middle Jurassic of Madagascar. *Bulletin de la Société Géologique de France* **176**: 467–473.
- Campos-Soto S, Benito MI, Cobos A, Caus E, Quijada IE, Suarez-Gonzalez P, Mas R, Royo-Torres R, Alcalá L. 2019.** Revisiting the age and palaeoenvironments of the Upper Jurassic–Lower Cretaceous? Dinosaur-bearing sedimentary record of eastern Spain: implications for Iberian palaeogeography. *Journal of Iberian Geology* **45**: 471–510.
- Carballido JL, Pol D. 2010.** The dentition of *Amygdalodon patagonicus* (Dinosauria: Sauropoda) and the dental evolution in basal sauropods. *Comptes Rendus Palevol* **9**: 83–93.
- Carey MA, Madsen JH. 1972.** Some observations on the growth, function, and differentiation of sauropod teeth from the Cleveland-Lloyd quarry. *Utah Academic Proceedings* **49**: 40–43.
- Casnovas ML, Santafé JV, Sanz JL. 2001.** *Losillasaurus giganteus*, un nuevo saurópodo del tránsito Jurásico–Cretácico de la cuenca de «Los Serranos» (Valencia, España). *Paleontologia i Evolució* **32–33**: 99–122.
- Chatterjee S, Zheng Z. 2005.** Neuroanatomy of *Shunosaurus*, a basal sauropod dinosaur from the Middle Jurassic of China. *Zoological Journal of the Linnean Society of London* **136**: 145–169.
- Cobos A, Royo-Torres R, Gascó F, Alcalá L. 2011.** A new giant turiasaurian specimen from Riodeva (Teruel, Spain). In: Van der Geer A, Athanassiou A, eds. *9th Annual Meeting of the European Association of Vertebrate Palaeontologists. Heraklion, Crete, Greece. Program and abstracts book, 8*. Heraklion: European Association of Vertebrate Palaeontologists.
- D’Emic MD. 2012.** The early evolution of titanosauriform sauropod dinosaurs. *Zoological Journal of the Linnean Society* **166**: 624–671.
- Gallina PA, Otero A. 2015.** Reassessment of *Laplataosaurus araukanicus* (Sauropoda: Titanosauria) from the Upper Cretaceous of Patagonia, Argentina. *Ameghiniana* **52**: 487–501.
- Goloboff PA. 2014.** Extended implied weighting. *Cladistics* **30**: 260–272.
- Goloboff PA, Catalano SA. 2016.** TNT version 1.5, including a full implementation of phylogenetic morphometrics. *Cladistics* **32**: 221–238.
- Goloboff PA, Farris JS, Nixon KC. 2008.** TNT, a free program for phylogenetic morphometrics. *Cladistics* **24**: 1–13.
- Harris JD. 2007.** The appendicular skeleton of *Suuwassea emiliae* (Sauropoda: Flagellicaudata) from the Upper Jurassic Morrison Formation of Montana (USA). *Geobios* **40**: 501–522.
- He X, Li K, Cai K. 1988.** *The Middle Jurassic dinosaur fauna from Dashanpu, Zigong, Sichuan: sauropod dinosaurs*. Omeisaurus tianfuensis. Chengdu: Sichuan Scientific and Technological Publishing House, 143. [In Chinese, English summary.]
- Holwerda FM, Pol D, Rauhut OWM. 2015.** Using dental enamel wrinkling to define sauropod tooth morphotypes from the Cañadón Asfalto Formation, Patagonia, Argentina. *PLoS One* **10**: e0118100.
- Huene FV. 1929.** Los saurisqueos y ornitisquios del Cretáceo Argentino. *Museo de la Plata, Anales* **3**: 194.
- Ikejiri T, Tidwell V, Trexler DL. 2005.** New adult specimens of *Camarasaurus lentus* highlight ontogenetic variation within species. In: Tidwell V, Carpenter K, eds. *Thunderlizards: the sauropodomorphs*. Berkeley: University California Press, 154–179.
- Janensch W. 1950.** Die Wirbelsäule von *Brachiosaurus brancai*. *Palaeontographica (suppl. 7)* **3**: 27–93.
- Janensch W. 1961.** Die Gliedmaszen und Gliedmaszengürtel der Sauropoden der Tendaguru-schichten. *Palaeontographica (Suppl. 7)* **3**: 177–235.
- Läng E. 2008.** *Les cétiosaures (Dinosauria, Sauropoda) et les sauropodes du Jurassiquemoyen: révisionsystématique, nouvellesdécouvertes et implications phylogénétiques*. Unpublished Ph.D Thesis, Muséum national d’Histoire naturelle, Paris.
- Läng E, Mahammed F. 2010.** New anatomical data and phylogenetic relationships of *Chebsaurusalgeriensis* (Dinosauria, Sauropoda) from the Middle Jurassic of Algeria. *Historical Biology* **22**: 142–164.
- Lapparent AF. 1960.** Les dinosauriens du ‘continental intercalaire’ du Sahara central. *Mémoires de la Société Géologique de France* **88A**: 1–57.
- Le Loeuff J, Métails E, Dutheil DB, Rubino JL, Buffetaut E, Lafont F, Cavin L, Moreau F, Tong H, Blanpied CH, Sbeta A. 2010.** An Early Cretaceous vertebrate assemblage from the Cabao Formation of NW Libya. *Geological Magazine* **147**: 750–759.
- Lemoine P. 1906.** Études géologiques dans le nord de Madagascar. In: Herman A, ed. *Contributions à l’histoire géologique de l’Océan Indien*. Paris: Librairie Scientifique, 1–520.
- Luque L, Cobos A, Royo-Torres R, Espílez E, Alcalá L. 2005.** Caracterización de los depósitos sedimentarios con dinosaurios de Riodeva (Teruel). *Geogaceta* **38**: 27–30.
- Mahammed F, Läng E, Mami L, Mekhali L, Benhamou M, Bouterfa B, Kacemi A, Cherief S-A, Chaouati H, Taquet P. 2005.** The ‘Giant of Ksour’, a Middle Jurassic sauropod dinosaur from Algeria. *Comptes Rendus Palevol* **4**: 707–714.
- Mannion PD. 2010.** A revision of the sauropod dinosaur genus ‘*Bothriospondylus*’ with a redescription of the type material of the Middle Jurassic form ‘*B. madagascariensis*’. *Palaeontology* **53**: 277–296.
- Mannion PD, Upchurch P, Mateus O, Barnes R, Jones MEH. 2012.** New information on the anatomy and systematic position of *Dinheirosaurus lourinhanensis* (Sauropoda: Diplodocoidea) from the Late Jurassic of Portugal, with a review of European diplodocoids. *Journal of Systematic Palaeontology* **168**: 98–206.
- Mannion PD, Upchurch P, Barnes RN, Mateus O. 2013.** Osteology of the Late Jurassic Portuguese sauropod dinosaur *Losotitan atalaiensis* (Macronaria) and the evolutionary

- history of basal titanosauriforms. *Zoological Journal of the Linnean Society* **168**: 98–206.
- Mannion PD, Allain R, Moine O. 2017.** The earliest known titanosauriform sauropod dinosaur and the evolution of Brachiosauridae. *PeerJ* **5**: e3217.
- Mannion PD, Upchurch P, Schwarz D, Wings O. 2019.** Taxonomic affinities of the putative titanosaurs from the Late Jurassic Tendaguru Formation of Tanzania: phylogenetic and biogeographic implications for eusauropod dinosaur evolution. *Zoological Journal of the Linnean Society* **185**: 784–909.
- Manuppella G, Antunes MT, Pais J, Ramalho MM, Rey J. 1999.** *Notícia explicativa da Folha 30A (Lourinhã)*. Lisboa: Departamento de Geologia do Instituto Geológico e Mineiro, 83.
- Marsh OC. 1878.** Principal characters of American Jurassic dinosaurs. Part I. *American Journal of Science Series 3* **16**: 411–416.
- Martill DM. 1988.** A review of the terrestrial vertebrate fossils of the Oxford Clay (Callovian–Oxfordian) of England. *Mercian Geologist* **11**: 171–190.
- Mateus O, Mannion PD, Upchurch P. 2014.** *Zby atlanticus*, a new turiasaurian sauropod (Dinosauria, Eusauropoda) from the Late Jurassic of Portugal. *Journal of Vertebrate Paleontology* **34**: 618–634.
- McIntosh JS. 1990.** Sauropoda. In: Weishampel DB, Dodson P, Osmólska H, eds. *The Dinosauria*. Berkeley: University of California Press, 345–390.
- McIntosh JS, Miller WE, Stadtman KL, Gillette DD. 1996.** The osteology of *Camarasaurus* Lewis (Jensen, 1988). *Brigham Young University Geology Studies* **41**: 73–115.
- Mocho P, Royo-Torres R, Ortega F, Malafaia E, Escaso F, Silva B. 2016.** Turiasauria-like teeth from the Upper Jurassic of the Lusitanian Basin, Portugal. *Historical Biology* **28**: 861–880.
- Mocho P, Royo-Torres R, Malafaia E, Escaso F, Ortega F. 2017a.** Sauropod tooth morphotypes from the Upper Jurassic of the Lusitanian basin (Portugal). *Papers in Palaeontology* **3**: 259–295.
- Mocho P, Royo-Torres R, Malafaia E, Escaso F, Ortega F. 2017b.** First occurrences of non-neosauropod eusauropod procoelous caudal vertebrae in the Portuguese Upper Jurassic record. *Geobios* **50**: 23–36.
- Mocho P, Royo-Torres R, Ortega F. 2019.** A new macronarian (Dinosauria, Sauropoda) from the Upper Jurassic of the Lusitanian Basin, Portugal. *Journal of Vertebrate Paleontology* **39**: e1578782.
- Moore AJ, Mo J, Clark JM, Xu X. 2018.** Cranial anatomy of *Bellusaurus sui* (Dinosauria: Eusauropoda) from the Middle–Late Jurassic Shishugou Formation of northwest China and a review of sauropod cranial ontogeny. *PeerJ* **6**: e4881.
- Ostrom JH, McIntosh JS. 1966.** *Marsh's dinosaurs. The collection from Como Bluff*. New Haven: Yale University Press, 388.
- Otero A. 2010.** The appendicular skeleton of *Neuquensaurus*, a Late Cretaceous saltasaurine sauropod from Patagonia, Argentina. *Acta Palaeontologica Polonica* **55**: 399–426.
- Otero A, Gallina PA, Canale JI, Haluza A. 2012.** Sauropod haemal arches: morphotypes, new classification and phylogenetic aspects. *Historical Biology* **24**: 243–256.
- Ouyang H, Ye Y. 2002.** *The first mamenchisaurian skeleton with complete skull: Mamenchisaurus youngi*. Chengdu: Sichuan Science and Technology Press, 110.
- Rauhut OWM, López-Arbarello A. 2009.** Considerations on the age of the Tiouaren Formation (Iullemeden Basin, Niger, Africa): implications for Gondwanan Mesozoic terrestrial vertebrate faunas. *Palaeogeography, Palaeoclimatology, Palaeoecology* **271**: 259–267.
- Riggs ES. 1903.** *Brachiosaurus altithorax*, the largest known dinosaur. *American Journal of Science* **15**: 299–306.
- Royo-Torres R, Upchurch P. 2012.** The cranial anatomy of the sauropod *Turiasaurus riodevensis* and implications for its phylogenetic relationships. *Journal of Systematic Palaeontology* **10**: 553–583.
- Royo-Torres R, Cobos A, Alcalá L. 2006.** A giant European dinosaur and a new sauropod clade. *Science* **314**: 1925–1927.
- Royo-Torres R, Cobos A, Aberasturi A, Espílez E, Fierro I, González A, Luque L, Mampel L, Alcalá L. 2009.** High European sauropod dinosaur diversity during Jurassic–Cretaceous transition in Riodeva (Teruel, Spain). *Palaeontology* **52**: 1009–1027.
- Royo-Torres R, Alcalá L, Cobos A. 2012.** A new specimen of the Cretaceous sauropod *Tastavinsaurus sanzi* from El Castellar (Teruel, Spain), and a phylogenetic analysis of the Laurasiformes. *Cretaceous Research* **34**: 61–83.
- Royo-Torres R, Upchurch P, Kirkland JI, DeBlieux DD, Foster JR, Cobos A, Alcalá L. 2017.** Descendants of the Jurassic turiasaurs from Iberia found refuge in the Early Cretaceous of western USA. *Scientific Reports* **7**: 14311.
- Saegusa H, Ikeda T. 2014.** A new titanosauriform sauropod (Dinosauria: Saurischia) from the Lower Cretaceous of Hyogo, Japan. *Zootaxa* **3848**: 1–66.
- Salgado L, de Carvalho IS. 2008.** *Uberabatitan ribeiroi*, a new titanosaur from the Marília Formation (Bauru Group, Upper Cretaceous), Minas Gerais, Brazil. *Palaeontology* **51**: 881–901.
- Salgado L, Coria RA, Calvo JO. 1997.** Evolution of titanosaurid sauropods. I: phylogenetic analysis based on the postcranial evidence. *Ameghiniana* **34**: 3–32.
- Schwarz D, Mannion PD, Wings O, Meyer CA. 2020.** Re-description of the sauropod dinosaur *Amanzia* ('*Ornithopsis/Cetiosauriscus*') *greppini* n. gen. and other vertebrate remains from the Kimmeridgian (Late Jurassic) Reuchenette Formation of Moutier, Switzerland. *Swiss Journal of Geosciences* **113**: 2.
- Sereno PC, Beck AL, Dutheil DB, Larson HCE, Lyon GH, Moussa B, Sadleir RW, Sidor CA, Varrichio DJ, Wilson GP, Wilson JA. 1999.** Cretaceous Sauropods from the Sahara and the uneven rate of skeletal evolution among dinosaurs. *Science* **286**: 1342–1347.
- Thevenin A. 1907.** Paléontologie de Madagascar. IV Dinosauriens. *Annales de Paléontologie* **2**: 121–136.
- Tidwell V, Carpenter K, Brooks W. 1999.** New sauropod from the Lower Cretaceous of Utah, USA. *Oryctos* **2**: 21–37.
- Tidwell V, Carpenter K, Meyer S. 2001.** New Titanosauriform (Sauropoda) from the Poison Strip Member

- of the Cedar Mountain Formation (Lower Cretaceous), Utah. In: Tanke DH, Carpenter K, eds. *Mesozoic Vertebrate Life*. Berkeley: Indiana University Press, 139–165.
- Tschopp E, Mateus O, Benson RBJ. 2015.** A specimen-level phylogenetic analysis and taxonomic revision of Diplodocidae (Dinosauria, Sauropoda). *PeerJ* **3**: e857.
- Upchurch P. 1995.** The evolutionary history of sauropod dinosaurs. *Philosophical Transactions of the Linnean Society* **124**: 43–103.
- Upchurch P. 1998.** The phylogenetic relationships of sauropod dinosaurs. *Zoological Journal of the Linnean Society* **124**: 43–103.
- Upchurch P, Barrett PM, Dodson P. 2004a.** Sauropoda. In: Weishampel DB, Dodson P, Osmolska H, eds. *The Dinosauria, 2nd edn*. Berkeley: University of California Press, 259–324.
- Upchurch P, Tomida Y, Barrett PM. 2004b.** A new specimen of *Apatosaurus ajax* (Sauropoda: Diplodocidae) from the Morrison Formation (Upper Jurassic) of Wyoming, USA. *National Science Museum Monographs* **26**: 1–107.
- Upchurch P, Mannion PD, Taylor MP. 2015.** The anatomy and phylogenetic relationships of ‘*Pelorosaurus*’ *becklesii* (Neosauropoda, Macronaria) from the Early Cretaceous of England. *PLoS One* **10**: e0125819.
- Wiersma K, Sander MP. 2017.** The dentition of a well-preserved specimen of *Camarasaurus* sp.: implications for function, tooth replacement, soft part reconstruction, and food intake. *PalZ* **91**: 145–161.
- Wilson JA. 2002.** Sauropod dinosaur phylogeny: critique and cladistic analysis. *Zoological Journal of the Linnean Society* **136**: 217–276.
- Wilson JA. 2005.** Redescription of the Mongolian sauropod *Nemegtosaurus mongoliensis* Nowinski (Dinosauria: Saurischia) and comments on Late Cretaceous sauropod diversity. *Journal of Systematic Palaeontology* **3**: 283–318.
- Wilson JA, Sereno PC. 1998.** Early evolution and higher-level phylogeny of sauropod dinosaurs. *Society of Vertebrate Paleontology Memoir* **5**: 1–68.
- Wilson JA, Upchurch P. 2009.** Redescription and reassessment of the phylogenetic affinities of *Euhelopus zdanskyi* (Dinosauria: Sauropoda) from the Late Jurassic or Early Cretaceous of China. *Journal of Systematic Palaeontology* **7**: 199–239.
- Xu X, Upchurch P, Mannion PD, Barrett PM, Regalado-Fernández OR, Mo J, Ma J, Liu H. 2018.** A new Middle Jurassic diplodocoid suggests an earlier dispersal and diversification of sauropod dinosaurs. *Nature Communications* **9**: 2700.
- Zaher H, Pol D, Carvalho AB, Nascimento PM, Riccomini C, Larson P, Juarez-Valieri R, Pires-Domingues R, da Silva NJ, de Almeida CD. 2011.** A complete skull of an Early Cretaceous sauropod and the evolution of advanced titanosaurs. *PLoS One* **6**: e16663.

SUPPORTING INFORMATION

Additional Supporting Information may be found in the online version of this article at the publisher’s web-site.

File S1. Institutional abbreviations. List of bones. Codification for the phylogenetic analyses. Information on the phylogenetic analyses including equal weights parsimony.

File S1, Figure S1. Strict consensus cladogram of extended implied weight analysis (with the same protocol as Mannion *et al.*, 2019) with the new specimen from San Lorenzo (Riodeva, Spain) separated from the *Losillasaurus*-type and new taxon *Narindasaurus thevenini*.

File S1, Figure S2. Strict consensus cladogram of conventional equal weights parsimony (same protocol as Mannion *et al.*, 2019 and Schwarz *et al.*, 2020) with the new specimen from San Lorenzo (Riodeva, Spain) and *Losillasaurus*-type in the same OTU and the new taxon *Narindasaurus thevenini*.

File S2. Key measurements.

File S3. *Losillasaurus giganteus* (San Lorenzo specimen) measurements.

File S4. *Narindasaurus thevenini* measurements.

File S5. Mesquite file.

File S6. TNT file.